CHAPTER 3

RESULTS AND DISCUSSION

3.1 Determination of Anionic Surfactants by Spectrophotometric Flow Injection Analysis involving On-line Solvent Extraction

The method used for the determination of anionic surfactants is based on an ion-pair extraction reaction with methylene blue (MB) in chloroform. It is usually reported for anionic surfactant contents as the amount of sodium dodecylsulphate (SDS). The anionic surfactant SDS reacts with MB to form an ion associate, which can be extracted into chloroform. The concentration of anionic surfactant can be determined by measuring the absorbance of the chloroform phase at 650 nm. Reaction scheme of dodecylsulphate (DS) and MB is shown as in Figure 3.1.

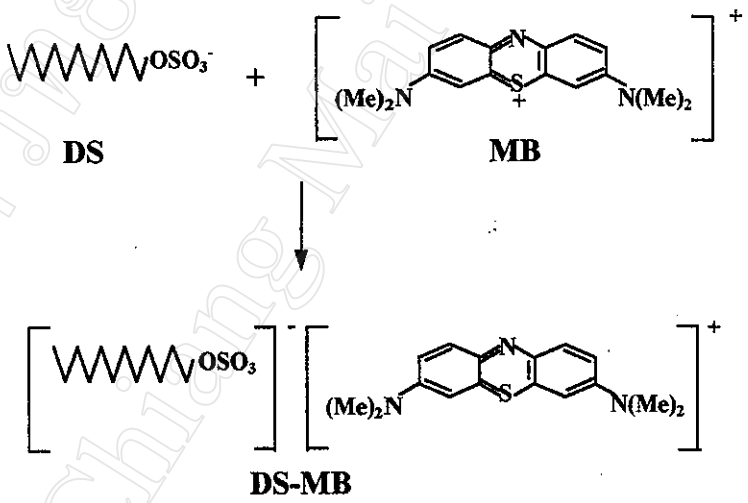

Figure 3.1 Reaction scheme of DS and MB [49]

The equilibrium of the DS, MB and DS-MB associated ion-pair in water and the chloroform phase have been qualitatively investigated [49]. The stability in the respective phase for each species was observed and examined. The DS dissolved in water was slightly soluble in chloroform. When chloroform was added onto the DS water solution, it became emulsified. Upon standing, it gradually became clear as time passed, and

DS transferred to the water phase, not to the chloroform phase. MB dissolved in chloroform (blue colour) as well as in water (blue colour). However, when water was added into MB chloroform solution, the blue colour of the chloroform phase rapidly transferred to the water phase, and after a few seconds of mixing, the colour in the chloroform phase disappeared. The fact that the DS-MB (1:1 molar ratio) associated ion pair in water is easily extracted to the chloroform phase is well known. This mentioned observation shows that DS molecules alone in the water phase never transfer to a chloroform phase, but only the associated ion pair of DS and MB can be extracted to the chloroform phase [49]. The equilibrium of these species can be shown as in Figure 3.2.

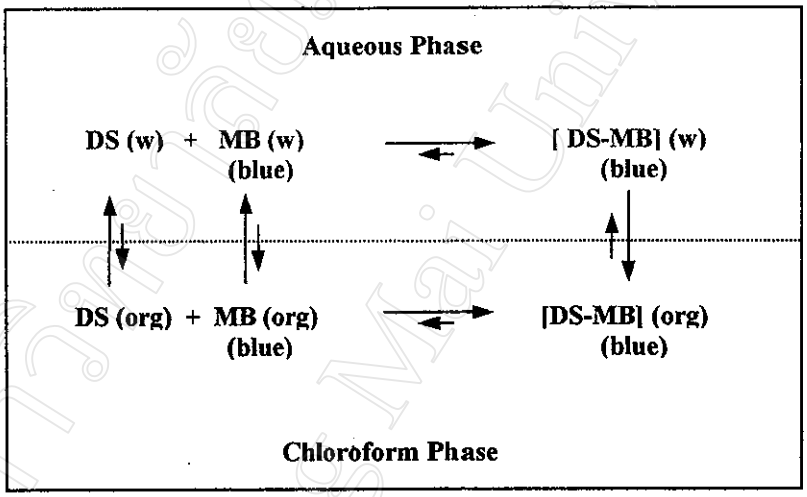

Figure 3.2 Equilibrium scheme of DS and MB in water and chloroform (organic) phase [49]

3.1.1 Preliminary Study of On-line Single Solvent Extraction

The FIA manifold with single solvent extraction for the determination of anionic surfactants was adapted from the QuikChem Method 10-306-00-1-A [66].

3.1.1.1 Manifold and Procedure

The FIA manifold involving on-line single solvent extraction for the determination of anionic surfactants was introduced by modifying the QuikChem 4200 (Lachat Instruments, WI, USA). The manifold is shown in Figure 3.3.

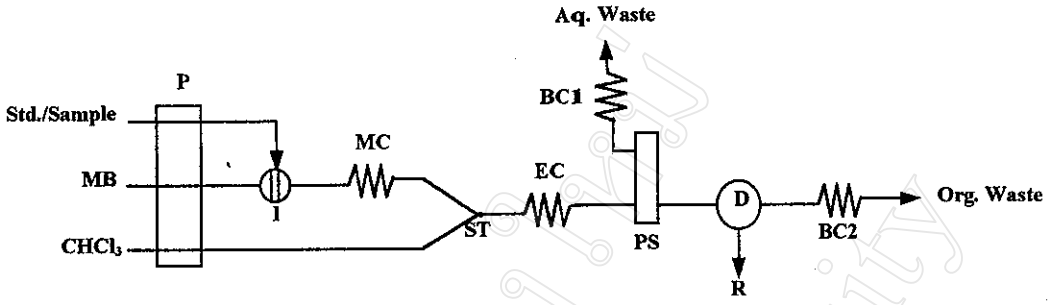

Figure 3.3 FIA manifold for the determination of anionic surfactants using single solvent extraction
P = peristaltic pump; I = injection valve; MC = mixing coil; ST = segmentor; EC = extraction coil; BC = back pressure coils; PS = PTFE membrane phase separator; D = spectrophotometer; R = chart recorder

The aqueous sample containing anionic surfactants is injected into an aqueous carrier stream (working methylene blue reagent solution). This stream is segmented with chloroform and the anionic surfactants are extracted over to the chloroform phase as ion pairs. The aqueous and chloroform phases are separated by a PTFE membrane phase separator. The absorbance of the chloroform stream is continuously measured at 650 nm, and is proportional to the amount of anionic surfactants.

3.1.1.2 Optimization

The manifold illustrated in Figure 3.3 was used. Preliminary conditions are presented in Table 3.1 for the optimization studied by varying one parameter while the others were kept constant.

Table 3.1 Preliminary conditions

Parameter	Condition
Working MB reagent solution	0.0038% (w/v) MB, 0.12 M KH_2PO_4 and 0.048 M K_2SO_4 in 0.034 M H_2SO_4
Sample volume	10 µl
MC	none
EC dimension	0.8 mm i.d. x 200 cm length
BC1 dimension	0.8 mm i.d. x 50 cm length
BC2 dimension	0.8 mm i.d. x 50 cm length
Flow-rate of working MB reagent	2.4 ml/min
Flow-rate of chloroform	2.0 ml/min
Analytical wavelength	630 nm
Full scale range of recorder	0.1 V
Chart speed of recorder	5 mm/min

3.1.1.2.1 Pre-equilibrated Chloroform

Chloroform was pre-equilibrated with deionized water before used to examine. Using this pre-equilibrated chloroform, the base line can be made smoothly. The pre-equilibrated chloroform was used for further studies.

3.1.1.2.2 Mixing Coil (MC) Length

The 0.8 mm i.d. PTFE tubing was examined to use as mixing coil. The results shown in Table 3.2 indicated that MC length was increased the peak height decreased. The MC was not necessary for further studies.

Table 3.2 Effect of the MC length

MC length (cm)	Peak height (mV) of 1.00 mg SDS/l	Average peak height (mV)
none	33.4, 34.2, 33.4	33.7
25	25.0, 25.9, 24.6	25.2

3.1.1.2.3 Segmentor

A mixing chamber was examined to use as segmentor and extraction place. The results shown in Table 3.3 indicated that the peak height was decreased when mixing chamber was used. The three-way connector was selected for further studies.

Table 3.3 Effect of segmentor

Segmentor	Speed (cycles/min)	Flow-rate (ml/min)		Peak height (mV) of 1.00 mg SDS/l	Average peak height (mV)
		MB	$CHCl_3$		
Three-way connector	-	2.4	2.0	43.0, 41.1, 42.1	42.1
Mixing chamber	-	2.4	2.0	17.8, 19.6, 20.1	19.2
	1000			18.7, 18.2, 19.6	18.8
	-	2.0	1.8	20.6, 19.6, 18.7	19.6
	1000			18.2, 18.7, 17.8	18.2
	-	1.6	1.6	13.1, 12.2, 12.2	12.5
	1000			18.7, 16.4, 17.8	17.6
	-	1.2	1.4	14.0, 13.1, 13.1	13.4
	1000			13.1, 15.0, 15.0	14.4

3.1.1.2.4 Flow-rate of Working MB Reagent and Chloroform Streams

The results shown in Table 3.4 and Figure 3.4 indicated that the peak height was not so much different when the flow-rate of working MB reagent and chloroform streams were used in range 2.0-2.8 and 1.8-2.2 ml/min respectively. The flow-rate of 2.4 ml/min for working MB reagent stream and 2.0 ml/min for chloroform stream were selected for the further studies.

Table 3.4 Effect of flow-rate of working MB reagent and chloroform streams

Flow-rate (ml/min)		Peak height (mV) of 1.00 mg SDS/l	Average peak height (mV)
MB	$CHCl_3$		
2.0	1.8	35.5, 33.2, 34.6	34.4
2.4	2.0	34.6, 34.6, 34.6	34.6
2.8	2.2	34.1, 34.1, 33.7	34.0

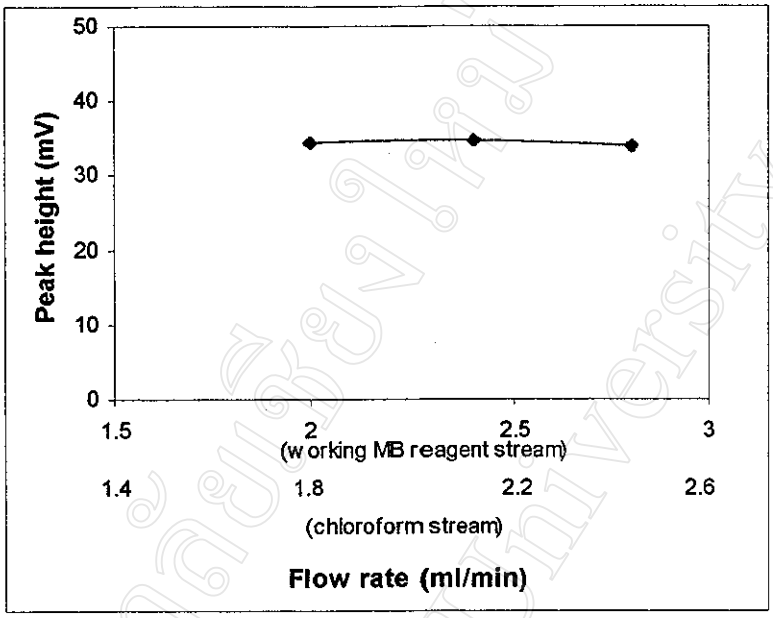

Figure 3.4 Effect of flow-rate of working MB reagent and chloroform streams

3.1.1.2.5 Extraction Coil (EC) Dimension

The results of an extraction coil dimension study are shown in Table 3.5 and Figure 3.5. It was found that the higher peak height was obtained when the extraction coil with 0.5 mm i.d. was used. The peak height was not quite different when the extraction coil with 0.5 mm i.d. was used in the range 50-200 cm length. The extraction coil with 0.5 mm i.d. and 50 cm length was chosen.

Table 3.5 Effect of extraction coil dimension

Extraction coil dimension		Peak height (mV) of 1.00 mg SDS/l	Average peak height (mV)
i.d. (mm)	Length (cm)		
0.8	22.5	19.6, 20.6, 20.1	20.1
	50	36.0, 37.4, 37.4	36.9
	100	39.3, 38.3, 37.4	38.3
	150	37.4, 37.4, 36.5	37.1
0.5	50	46.8, 45.8, 46.8	46.5
	100	47.7, 48.6, 47.7	48.0
	150	48.6, 48.6, 47.7	48.3
	200	45.8, 46.8, 45.8	46.1

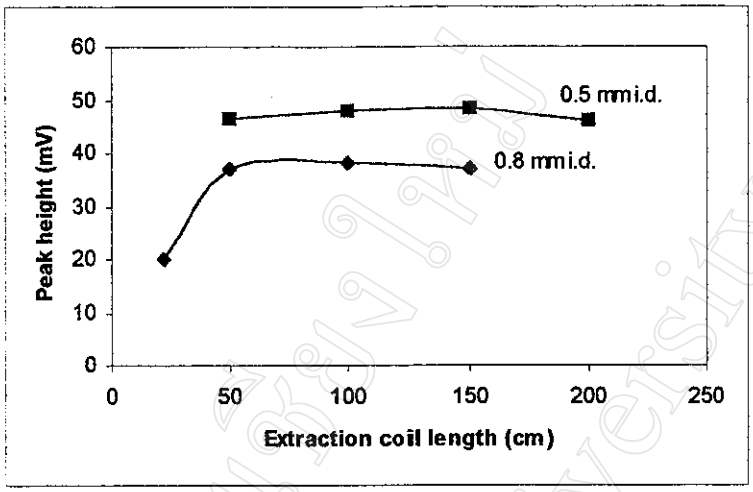

Figure 3.5 Effect of extraction coil dimension

3.1.1.2.6 Analytical Wavelength

The results shown in Table 3.6 indicated that the higher peak height was obtained when the absorbance was measured at 650 nm, the same as previously reported [49]. The analytical wavelength at 650 nm was selected for the further studies.

Table 3.6 Effect of analytical wavelength

Analytical Wavelength (nm)	Peak height (mV) of 1.00 mg SDS/l	Average peak height (mV)
630	36.5, 38.3, 38.3	37.7
650	123.4, 123.4, 123.4	123.4

3.1.1.2.7 Sample Volume

The results of a sample volume study are shown in Table 3.7 and Figure 3.6. It was found that the higher sample volume, the higher peaks obtained. The sample volume of 50 µl was therefore chosen for further studies.

Table 3.7 Effect of sample volume

Sample volume (µl)	Peak height* (mV) of	
	0.05 mg SDS/l	0.30 mg SDS/l
10	3.7	33.0
30	7.2	44.4
40	12.9	72.5
50	20.9	126.5
60	19.4	124.4

*Mean of triplicate injections

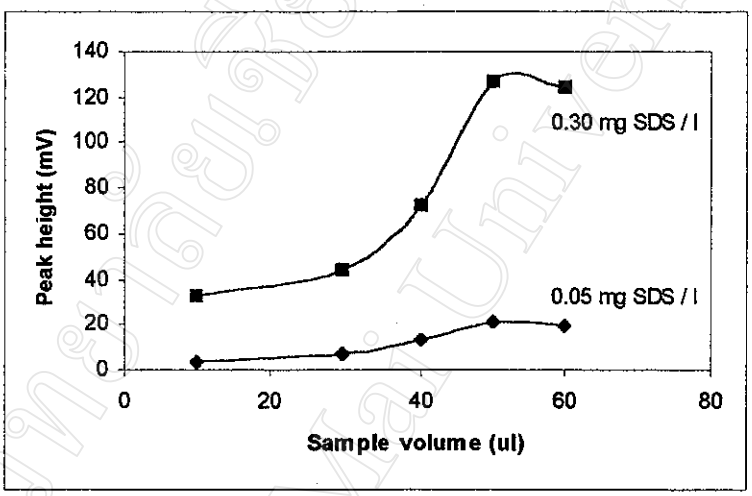

Figure 3.6 Effect of sample volume

3.1.1.3 Summary of the Optimum Conditions

A diagram of the purposed FIA manifold is displayed in Figure 3.3 and the optimum conditions are summarized in Table 3.8.

Table 3.8 Optimum conditions for FIA system with single solvent extraction

Parameter	Condition
Working MB reagent solution	0.0038% (w/v) MB, 0.12 M KH_2PO_4 and 0.048 M K_2SO_4 in 0.034 M H_2SO_4
Sample volume	50 µl
MC	none
EC dimension	0.5 mm i.d. x 50 cm length
BC1 dimension	0.8 mm i.d. x 50 cm length
BC2 dimension	0.8 mm i.d. x 50 cm length
Flow-rate of working MB reagent	2.4 ml/min
Flow-rate of chloroform	2.0 ml/min
Analytical wavelength	650 nm
Full scale range of recorder	0.5 V
Chart speed of recorder	5 mm/min

3.1.1.4 Calibration Graph and Detection Limit

The optimum conditions obtained in section 3.1.1.3 were used to produce a calibration graph. Results are shown in Table 3.9, Figures 3.7 and 3.8. From the calibration graph, detection limit ($3s_B$) [232] was also calculated as 0.04 mg SDS/l.

Table 3.9 Peak height of standard SDS solutions

Std. solutions conc. (mg SDS/l)	Peak height* (mV)	Calibration graph
0.025	3.1	$y = 314.5\ (x) - 0.401$ $r^2 = 0.9986$
0.05	10.9	
0.10	35.8	
0.20	62.3	
0.30	93.4	
0.40	130.4	
0.50	163.5	
0.60	189.2	
0.70	217.6	
0.80	246.8	
0.90	278.8	
1.00	316.9	

*Mean of triplicate injections

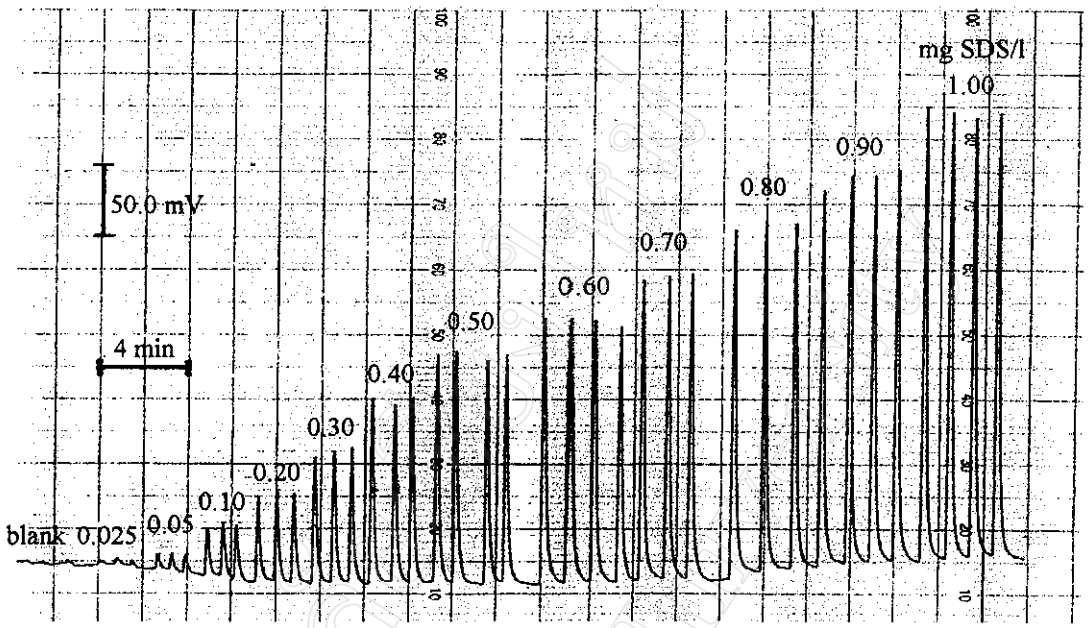

Figure 3.7 FIA-gram of standard SDS solutions

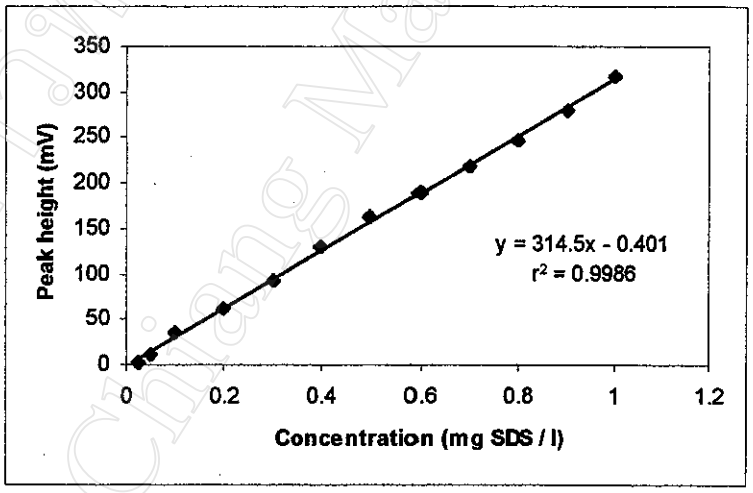

Figure 3.8 Calibration graph of FI single solvent extraction for the determination of anionic surfactants

3.1.1.5 Precision

Using the optimum conditions summarized in section 3.1.1.3, precision was determined by repeating injection of a standard solution (0.10 mg SDS/l) for 9 replicates. The results shown in Table 3.10

indicated that the relative standard deviation (RSD) of 3.8% was obtained.

Table 3.10 Precision study

Standard SDS solution (mg SDS/l)	Peak height (mV)	$\bar{X}$ (mV)	SD	%RSD
0.10	39.3, 38.3, 38.3, 41.1, 37.4, 36.5, 40.2, 39.3, 40.2	39.0	1.5	3.8

3.1.1.6 Percentage Recovery

The percentage recovery was studied by spiking various amounts of SDS standard solutions (0.02-0.10 mg SDS/l) into water sample. The optimum conditions summarized in section 3.1.1.3 were used. The results shown in Tables 3.11 (a) and (b) indicated that the average percentage recovery of 100% was obtained when this recommended FIA procedure was applied to determine anionic surfactant contents in natural water sample (from Ang-Kaew reservoir, Chiang Mai Campus).

Table 3.11 (a) Peak height of standard SDS solutions

SDS standard solution (mg SDS/l)	Peak height* (mV)	Calibration graph
0.02	1.9	$y = 367.0\ (x) - 5.040$ $r^2 = 0.9968$
0.04	10.3	
0.06	16.4	
0.08	25.1	
0.10	31.2	

*Mean of triplicate injections

Table 3.11 (b) Percentage recovery

SDS added (mg SDS/l)	SDS found		SDS found (mg SDS/l) corrected for sample	Recovery (%)
	peak height* (mV)	(mg SDS/l)		
0	8.0	0.03	-	-
0.02	14.3	0.05	0.02	100
0.04	22.1	0.07	0.04	100
0.06	27.4	0.09	0.06	100
0.08	33.9	0.11	0.08	100
0.10	40.8	0.13	0.10	100

*Mean of triplicate injections

3.1.2 On-line Double Solvent Extraction

According to Abbott's method [43], which is a batch procedure, double extraction should overcome interferences in a real sample. Further investigation was then made using FIA system with double solvent extraction. The methylene blue-anionic surfactant ion associate is partitioned into chloroform from an alkaline methylene blue solution to avoid the negative interference of proteinaceous material present in environmental samples. The chloroform phase is then back-extracted with an acidified methylene blue solution in order to remove the interference of those materials such as inorganic anions, eg nitrate, chloride etc., that form methylene blue complexes of low chloroform extractability.

3.1.2.1 Manifold and Procedure

The preliminary study of a FIA method with single solvent extraction (section 3.1.1) was useful for the first designation of a FIA manifold with double solvent extraction. The on-line double solvent extraction manifold for the determination of anionic surfactants was introduced by modifying the previous single extraction device and QuikChem 4200 (Lachat Instruments, WI, USA). The manifold is illustrated in Figure 3.9.

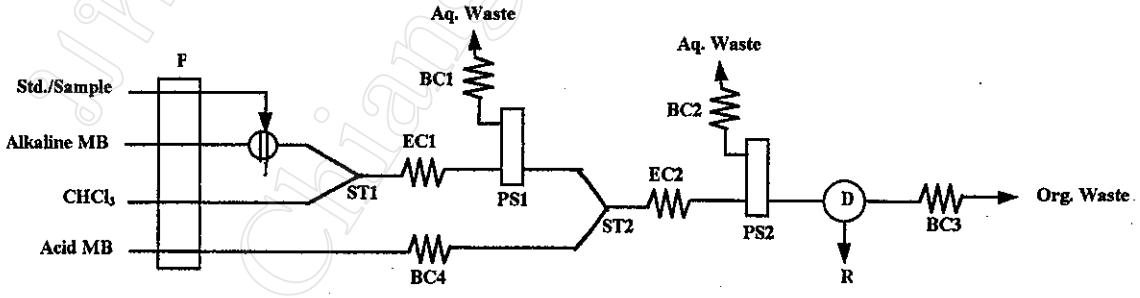

Figure 3.9 FIA manifold for the determination of anionic surfactants using double solvent extraction
P = peristaltic pump; I = injection valve; ST = segmentor;
EC = extraction coils; BC = back pressure coils;
PS = PTFE membrane phase separator;
D = spectrophotometer; R = chart recorder

A standard or sample is injected via an injection valve into the stream of alkaline methylene blue solution. This stream is merged with a chloroform stream to create segments by a segmentor (ST1). The extraction takes place during the segments passing the extraction coil (EC1), until reaching a phase separator (PS1) where the chloroform phase is separated out and flowing further to merge with the stream of acid methylene blue at another segmentor (ST2). Extraction takes place again during the passage through the extraction coil (EC2). The phase separator (PS2) separates the chloroform phase out and the chloroform stream flows through the flow-cell to be monitored continuously at 650 nm.

3.1.2.2 Optimization

The manifold illustrated in Figure 3.9 was used. Preliminary conditions are shown in Table 3.12 for the optimization studied by varying one parameter while the others were kept constant.

Table 3.12 Preliminary conditions

Parameter	Condition
Alkaline MB solution	0.0015% (w/v) MB and 0.0075 M $Na_2B_4O_7$ in 0.015 M NaOH
Acid MB solution	0.0010% (w/v) MB, $5.0x10^{-4}$ M $Na_2B_4O_7$ and $1.0x10^{-3}$ M NaOH in $5.0x10^{-3}$ M H_2SO_4
EC1 dimension	0.5 mm i.d. x 50 cm length
EC2 dimension	0.5 mm i.d. x 50 cm length
BC1 dimension	0.8 mm i.d. x 50 cm length
BC2 dimension	0.8 mm i.d. x 50 cm length
BC3 dimension	0.8 mm i.d. x 50 cm length
BC4 dimension	none
Sample volume	50 µl
Flow-rate of alkaline MB solution	2.4 ml/min
Flow-rate of chloroform	2.0 ml/min
Flow-rate of acid MB solution	1.4 ml/min
Analytical wavelength	650 nm
Full scale range of recorder	0.2 V
Chart speed of recorder	5 mm/min

3.1.2.2.1 Back Pressure Coil

When the first condition described in section 3.1.2.2 was used. It was found that after the chloroform phase was separated by phase separator (PS1), this chloroform stream could not further flow to merge with the stream of acid methylene blue at ST2. BC1 (0.8 mm i.d. x 50 cm length) was changed to use another one with smaller i.d. and longer length (0.5 mm i.d. x 150 cm length). BC4 (0.5 mm i.d. x 100 cm length) was also added, in order to optimize pressure so the chloroform stream can further flow to merge with the stream of acid methylene blue and segmentation was created. BC1 (0.5 mm i.d. x 150 cm) and BC4 (0.5 mm i.d. x 100 cm) were used for the further studies.

3.1.2.2.2 Pre-equilibrated Chloroform

Chloroform was pre-equilibrated with water before used to examine. The results shown in Table 3.13 and Figure 3.10 indicated that the higher peak height the smoother base line could be obtained by using the pre-equilibrated chloroform. The pre-equilibrated chloroform was used for further studies.

Table 3.13 Effect of pre-equilibrated chloroform

SDS standard solution (mg SDS/l)	Peak height* (mV)	
	Non-equilibrated chloroform	Pre-equilibrated chloroform
0.06	-	2.6
0.08	6.7	7.1
0.10	12.3	15.0
0.20	28.0	33.3
0.40	56.7	68.1
0.60	84.2	104.1
0.80	117.5	133.7
1.00	139.8	154.0
Calibration graph	$y = 145.3x - 2.396$	$y = 165.0x - 2.091$
r^2	0.9980	0.9915

*Mean of triplicate injections

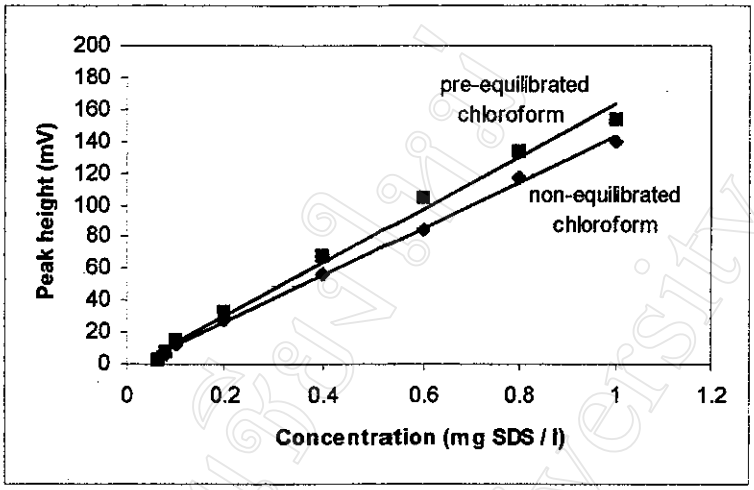

Figure 3.10 Effect of pre-equilibrated chloroform

3.1.2.2.3 Methylene Blue Concentration

This was studied by varying concentration of stock methylene blue solution. The results are shown in Table 3.14 and Figure 3.11. It was found that the higher concentrations of stock methylene blue solution, the higher peak obtained. The peak height was decreased when stock MB solution was used at concentration of 0.100% (w/v). The 0.050% (w/v) stock methylene blue was chosen for the further studies.

Table 3.14 Effect of methylene blue concentration

Stock MB solution concentration (% w/v)	MB concentration (% (w/v))		Peak height* (mV) of standard solution (mg SDS/l)				Calibration graph	r^2
	alkaline MB solution	acid MB solution	0.10	0.20	0.40	0.60		
0.006	3.8×10^{-4}	2.5×10^{-4}	6.6	26.0	50.0	76.9	$y = 136.7x - 4.551$	0.9939
0.012	7.5×10^{-4}	5.0×10^{-4}	9.4	28.0	55.6	85.1	$y = 148.9x - 3.859$	0.9978
0.025	1.5×10^{-3}	1.0×10^{-3}	5.6	23.8	51.9	82.3	$y = 151.1x - 8.214$	0.9985
0.050	3.0×10^{-3}	2.0×10^{-3}	14.0	31.8	63.6	93.5	$y = 158.4x - 0.741$	0.9990
0.100	6.0×10^{-3}	4.0×10^{-3}	8.9	22.0	47.7	71.0	$y = 126.3x - 3.388$	0.9997

*Mean of triplicate injections

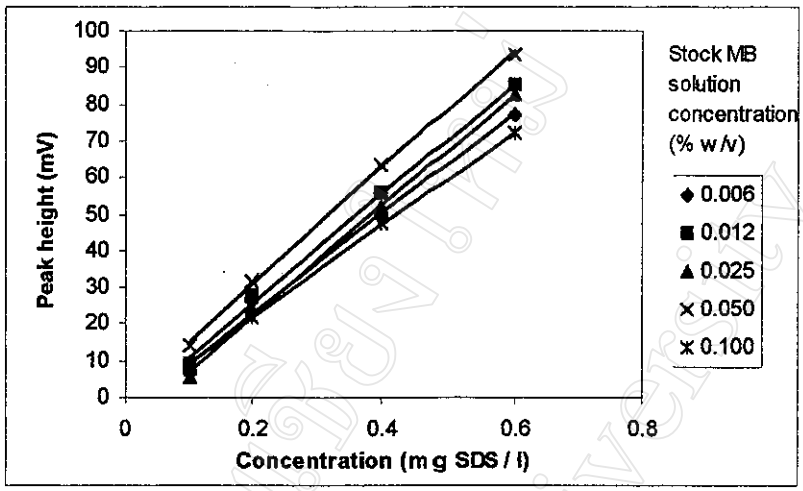

Figure 3.11 Effect of methylene blue concentration

3.1.2.2.4 Sample Volume

The results of a sample volume study are shown in Table 3.15 and Figure 3.12. It was found that the sample volume was increased the peak height increased. The broad peak was also obtained when sample volume was increased. The sample volume of 150 µl was selected for the further studies.

Table 3.15 Effect of sample volume

Sample volume (µl)	Peak height* (mV) of standard solution (mg SDS/l)					Calibration graph	r^2
	0.02	0.04	0.06	0.08	0.10		
50	0.9	2.3	5.0	6.8	9.4	y = 107.5x – 1.570	0.9914
100	3.0	7.2	11.4	17.1	21.3	y = 232.5x – 1.950	0.9969
150	5.5	10.8	17.0	22.3	28.8	y = 290.5x – 0.550	0.9989
200	5.5	15.0	30.2	39.7	42.4	y = 492.5x – 2.990	0.9569

*Mean of triplicate injections

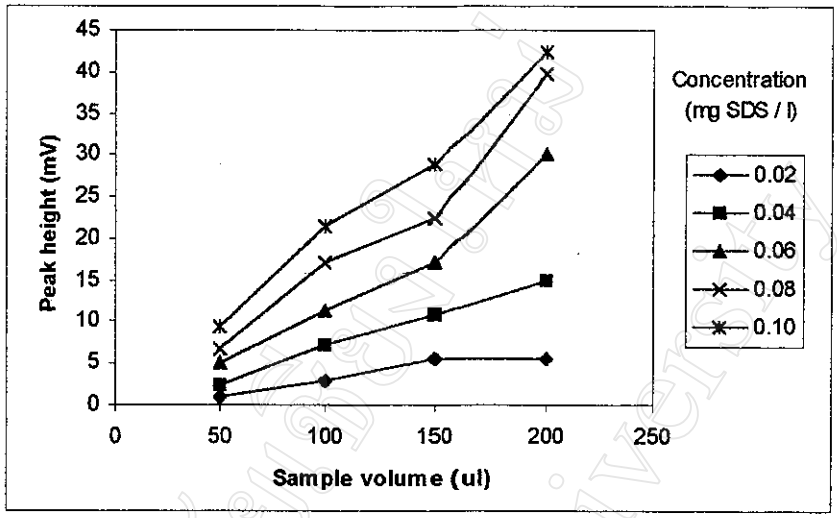

Figure 3.12 Effect of sample volume

3.1.2.2.5 Membrane Pore Size

The PTFE membranes with different pore size were examined. The results are shown in Table 3.16 and Figure 3.13. It can be observed that using the same type of PTFE membrane (Zitex) but different pore sizes, the ones with the smaller pore size, the lower peaks obtained. The Millipore (pore size = 10 μm) was chosen when using this optimized condition. The PTFE membranes with different pore size can be used, however, the flow-rates of reagents and chloroform should be optimized.

Table 3.16 Effect of membrane pore size

Standard solution (mg SDS/l)	Peak height* (mV)			
	Type of membrane			
	Millipore	Zitex A145	Zitex A150	Zitex A155
0.06	10.1	6.9	3.7	5.0
0.08	14.6	11.2	6.4	7.8
0.10	20.1	16.8	8.0	12.6
0.20	40.5	36.5	19.8	26.3
0.40	94.6	83.5	45.5	62.3
0.60	150.3	128.7	56.1	96.2
0.80	194.5	166.2	81.4	135.3
1.00	223.7	199.7	95.7	171.7
Calibration graph	y = 238.0x–2.860	y = 209.9x-3.811	y = 99.1x-0.555	y = 176.9x-6.980
r^2	0.9939	0.9973	0.9922	0.9991
Pore size (μm)	10	10-20	5-10	2-5
Time per one injection (min)	2	2	3	4

*Mean of triplicate injections

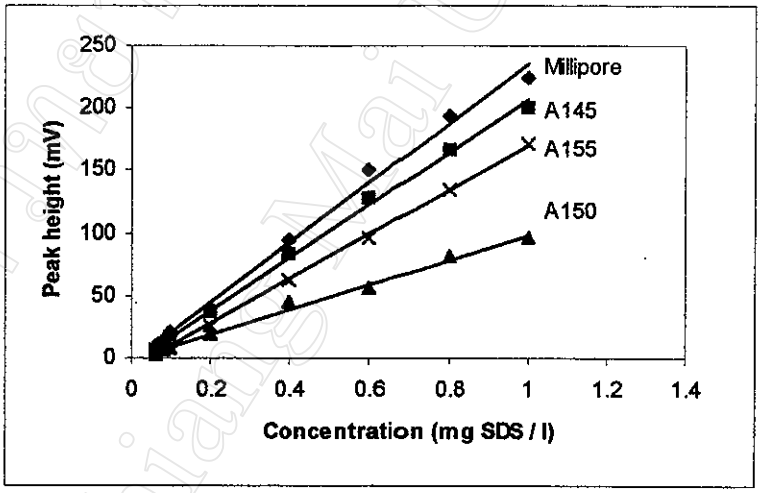

Figure 3.13 Effect of membrane pore size

3.1.2.3 Summary of the Optimum Conditions

The recommended FIA manifold with double solvent extraction for the determination of anionic surfactants in waters is displayed in Figure 3.9 and the summary of the optimum conditions are shown in Table 3.17.

Table 3.17 Optimum conditions for FIA system with double solvent extraction

Parameter	Condition
Alkaline MB solution	0.0030% (w/v) MB and 0.0075 M $Na_2B_4O_7$ in 0.015 M NaOH
Acid MB solution	0.0020% (w/v) MB, 5.0×10^{-4} M $Na_2B_4O_7$ and 1.0×10^{-3} M NaOH in 5.0×10^{-3} M H_2SO_4
EC1 dimension	0.5 mm i.d. x 50 cm length
EC2 dimension	0.5 mm i.d. x 50 cm length
BC1 dimension	0.5 mm i.d. x 150 cm length
BC2 dimension	0.8 mm i.d. x 50 cm length
BC3 dimension	0.8 mm i.d. x 50 cm length
BC4 dimension	0.5 mm i.d. x 100 cm length
Sample volume	150 µl
Flow-rate of alkaline MB solution	2.4 ml/min
Flow-rate of chloroform	2.0 ml/min
Flow-rate of acid MB solution	1.4 ml/min
Analytical wavelength	650 nm
Full scale range of recorder	0.2 V
Chart speed of recorder	5 mm/min

3.1.2.4 Calibration Graph and Detection Limit

The conditions described in section 3.1.2.3 were used to perform a calibration graph and to estimate the detection limit. The results are shown in Table 3.18, Figures 3.14 and 3.15. The detection limit ($3s_B$) [232] was calculated as 0.02 mg SDS/l.

Table 3.18 Peak height of standard SDS solutions

Standard SDS concentration (mg SDS/l)	Peak height* (mV)	Calibration graph
0.02	0.0	$y = 238.3x - 2.321$ $r^2 = 0.9982$
0.04	7.0	
0.06	13.8	
0.08	17.5	
0.10	21.6	
0.20	45.9	
0.40	92.4	

*Mean of quadruplicate injections

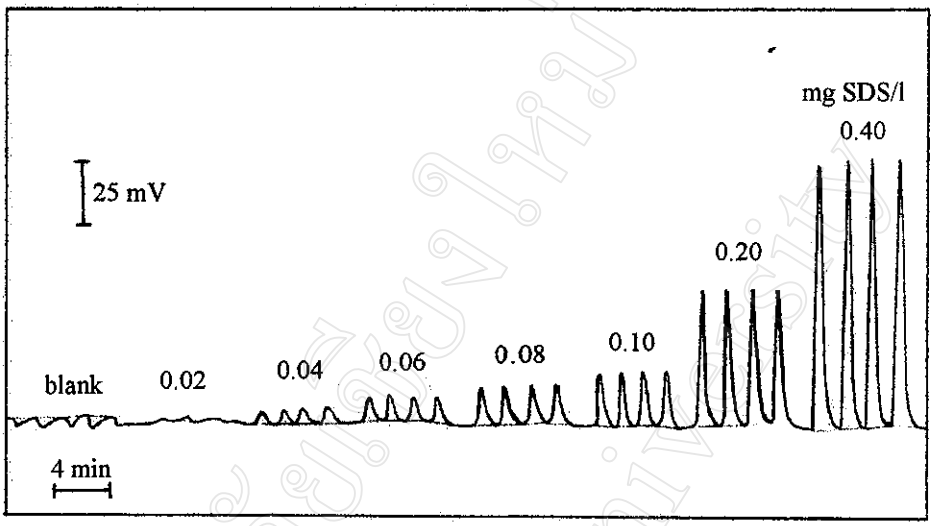

Figure 3.14 FIA-gram of standard SDS solutions

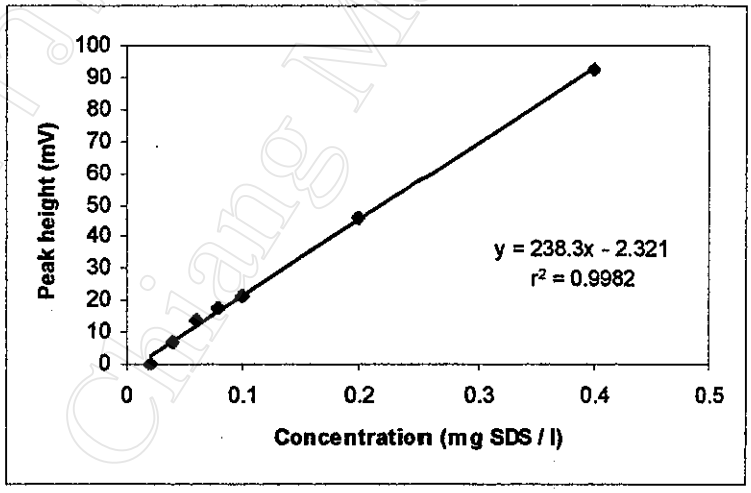

Figure 3.15 Calibration graph

3.1.2.5 Precision

The precision was examined by repeating injection of standard solutions (0.04 and 0.40 mg SDS/l) and sample from Chiang Mai moat (site 1) for 21 replicates each using the optimum conditions summarized in section 3.1.2.3. The results shown in Table 3.19 indicated that the relative standard deviations (RSD) of 8.4%, 1.3% and 7.7% were obtained respectively.

Table 3.19 Precision study

Standard SDS solution (mg SDS/l)	Peak height (mV)	$\bar{X}$ (mV)	SD	%RSD
0.04	7.0, 6.6, 8.4, 6.6, 6.6, 7.0, 7.0, 6.6, 8.0, 7.0, 7.5, 7.0, 7.0, 7.0, 7.5, 8.0, 6.6, 7.0, 8.0, 5.6, 6.6	7.1	0.6	8.4
0.40	95.8, 96.9, 96.9, 99.3, 98.1, 96.9, 96.9, 100.4, 98.1, 95.8, 96.9, 99.3, 96.9, 96.9, 98.1, 96.9, 95.8, 98.1, 96.9, 95.8, 95.8	97.3	1.3	1.3
Sample from Chiang Mai moat (site 1)	17.3, 20.6, 23.4, 21.0, 22.0, 18.7, 20.6, 18.2, 19.6, 18.7, 16.8, 19.6, 18.7, 18.7, 19.6, 18.7, 19.1, 18.7, 18.7, 19.6, 19.6	19.4	1.5	7.7

3.1.2.6 Interference Study

The effect of interfering ions was studied by adding interfering ions into 0.10 mg SDS/l standard solution. Interference is considered to occur when the obtained peak height is outside the range $\bar{x} \pm 2SD$, where $\bar{x}$ is the response due to 0.10 mg SDS/l alone. Results are shown in Table 3.20. It was found that the following species: urea, NH_4^+, NO_3^-, S^{2-}, Cl^- and SO_4^{2-} did not interfere the determination of SDS (0.10 mg/l) when the concentrations did not exceed 1000, 100, 100, 100, 1000 and 500 mg/l respectively.

Table 3.20 Interference study

Ion added	Added chemical form	Concentration added (mg/l)	Average peak height* (mV)	%Relative error
none	-	-	20.6#	-
urea	H_2NCONH_2	100	22.4	+8.7
		200	23.0	+11.7
		400	20.9	+1.4
		600	21.4	+3.9
		1000	18.7	-9.2
NH_4^+	NH_4Cl	80	21.4	+3.9
		100	22.8	+10.7
		300	26.6	+29.1
NO_3^-	$NaNO_3$	80	20.3	-1.5
		100	22.7	+10.2
		300	25.7	+21.4
S^{2-}	Na_2S	100	20.8	+1.0
		300	25.7	+24.8
Cl^-	NaCl	1000	18.2	-11.6
SO_4^{2-}	Na_2SO_4	300	20.8	+1.0
		400	21.6	+4.9
		500	20.2	-1.9
		1000	15.4	-25.2

*Mean of triplicate injections

$\bar{x} \pm 2(SD) = 20.6 \pm 2(2.4) = 15.8 - 25.4$ mV (n = 11)

3.1.2.7 Determination of Anionic Surfactants in Water Samples

The different types of water were collected. Addition of 1% (v/v) of a 40% formaldehyde solution to a water sample is required for storage [43]. The optimum conditions in section 3.1.2.3 were used to determine anionic surfactants in these water samples. The results are shown in Table 3.21. A comparative determination of anionic surfactants by Abbott's method (batch procedure) [43] was also carried out. The differences between the means obtained from the proposed method and the reference method were evaluated by t-test. The calculated t-test value of the proposed-FIA and batch methods was 0.259. The critical value of t-test is 2.132 (4 degrees of freedom) at the confidence internal of 90% [232], indicating that the results obtained by the recommended method were not significantly different from those obtained by the reference method with confidence interval of 90%.

Table 3.21 Application of the FIA procedure developed to different types of water

Water sample	Conc. of anionic surfactants (as mg SDS/l)	
	Abbott's method (batch procedure)	FIA
Sewage canal	2.40	2.32
Chiang Mai moat		
- Site 1	ND*	0.09
- Site 2	ND*	0.04
- Site 3	ND*	0.07
- Site 4	ND*	0.03
- Site 5	ND*	0.03
River	0.36	0.32
Pond	0.37	0.27
Inlet sewage pond	0.60	0.76
Outlet sewage pond	0.45	0.45

* Absorbance values are about the blank

3.1.2.8 Percentage Recovery

Various amounts of SDS standard solutions were spiked into samples, which were then analyzed to estimate the percentage recoveries. The results are presented in Table 3.22. It was found that using the proposed FIA procedure and Abbott's method, the percentage recoveries of from 100 to 120% and from 80 to 120% were obtained respectively.

Table 3.22 Percentage recovery

SDS standard solution added (mg SDS/l)	Anionic surfactants found					
	FIA			Abbott's method (batch procedure)		
	as mg SDS/l	corrected for sample (mg SDS/l)	% recovery	as mg SDS/l	corrected for sample (mg SDS/l)	% recovery
Chiang Mai moat (site 1)						
-	0.08	-	-	-	-	-
0.05	0.14	0.06	120	-	-	-
0.10	0.18	0.10	100	-	-	-
0.20	0.29	0.21	105	-	-	-
Chiang Mai moat (site 3)						
-	0.06	-	-	0.04	-	-
0.05	0.11	0.05	100	0.08	0.04	80
0.10	0.16	0.10	100	0.16	0.12	120
0.20	0.28	0.22	110	0.27	0.23	115
			$\bar{x}$ = 103			$\bar{x}$ = 105

3.1.2.9 Sample Pretreatment Method

Perhaps, sample pretreatment was necessary to isolate the precipitates. Three different methods; using filter paper, PTFE membrane and centrifugation were examined. The optimum conditions in section 3.1.2.3 were used. The results are shown in Table 3.23. It was found that centrifugation which resulted good reproducibility should be used. The water samples was centrifuged before the clear upper portion in the centrifuge tube was suctioned into the sample loop of the injection valve.

Table 3.23 Effect of sample pretreatment method

Sample pretreatment method	Repeat No.	Conc. of anionic surfactants (as mg SDS/l) in water		
		Pond	Inlet sewage pond	Outlet sewage pond
Filtrated through filter paper (Whatman No.42)	1	0.27	0.76	0.45
	2	0.55	1.10	0.56
	3	0.18	0.39	0.26
Filtrated through PTFE membrane (Sartorius, pore size = 0.45 μm)	1	0.70	0.79	0.75
	2	0.22	0.55	0.33
Centrifugation (DYNAC, speed = 80, 10 min)	1	0.20	0.85	0.35
	2	0.21	0.85	0.30
	3	0.21	0.83	0.31
	4	0.21	0.85	0.28
	5	0.23	0.89	0.37

3.2 Determination of Hyoscine Butylbromide by Spectrophotometric Flow Injection Analysis involving On-line Solvent Extraction

The extraction spectrophotometry is a general procedure for the estimation of quaternary ammonium compounds in drugs. In practice, a buffered aqueous solution containing quaternary ammonium compound and a suitable indicator dye is shaken with an organic solvent, and the concentration of the resulting ion-pair in the organic phase is determined spectrophotometrically. The hyoscine butylbromide (quaternary ammonium compound) formed an ion association compound with bromothymol blue (indicator dye) which is extracted into chloroform and measurement of the yellow colour in the chloroform is made spectrophotometrically at 420 nm [79].

3.2.1 Manifold and Procedure

The on-line solvent extraction manifold for the determination of hyoscine butylbromide was introduced by modifying the QuikChem 4200 (Lachat Instrument, WI, USA). The manifold is shown in Figure 3.16.

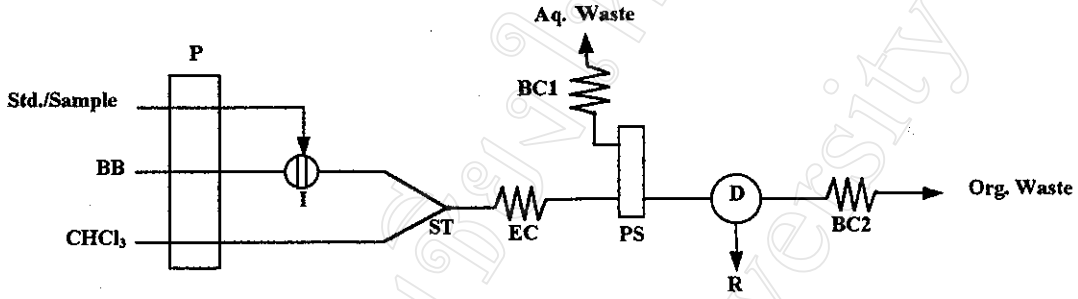

Figure 3.16 FIA manifold for the determination of HB using on-line solvent extraction
P = peristaltic pump; I = injection valve; ST = segmentor; EC=extraction coil; PS=PTFE membrane phase separator; BC = back pressure coils; D = spectrophotometer; R = chart recorder; BB = bromothymol blue

The standard solution or sample is injected into a buffer solution carrier stream. This stream is merged with a chloroform stream to create segments by a segmentor. The hyoscine butylbromide formed an ion pair with bromothymol blue, which is extracted into chloroform. The aqueous and chloroform phases are separated by a PTFE membrane phase separator. The absorbance of the chloroform stream is measured continuously at 420 nm, and is proportional to the amount of hyoscine butylbromide.

3.2.2 Optimization

The FIA manifold appeared in Figure 3.16 was used. Preliminary conditions are displayed in Table 3.24 for the optimization studied by varying one parameter while the others were kept constant.

Table 3.24 Preliminary conditions

Parameter	Condition
Bromothymol blue reagent solution	0.024% (w/v) BB in phosphate buffer (pH 7.5)
Sample volume	50 µl
EC dimension	0.5 mm i.d. x 50 cm length
BC1 dimension	0.8 mm i.d. x 50 cm length
BC2 dimension	0.8 mm i.d. x 50 cm length
Flow-rate of BB reagent solution	0.8 ml/min
Flow-rate of chloroform	2.0 ml/min
Analytical wavelength	420 nm
Full scale range of recorder	1 V
Chart speed of recorder	5 mm/min

3.2.2.1 Pre-equilibrated Chloroform

Chloroform was pre-equilibrated with water before used to examine. The results are displayed in Table 3.25 and Figure 3.17. The higher peak height and smooth base line can be obtained by using the pre-equilibrated chloroform. The pre-equilibrated chloroform was chosen for further studies.

Table 3.25 Effect of pre-equilibrated chloroform

HB standard solution (mg HB/l)	Peak height* (mV)	
	Non-equilibrated chloroform	Pre-equilibrated chloroform
50	86	112
100	174	209
200	291	329
Calibration graph	y = 1.339x + 27.5	y = 1.411x + 52.0
r^2	0.9882	0.9834

*Mean of triplicate injections

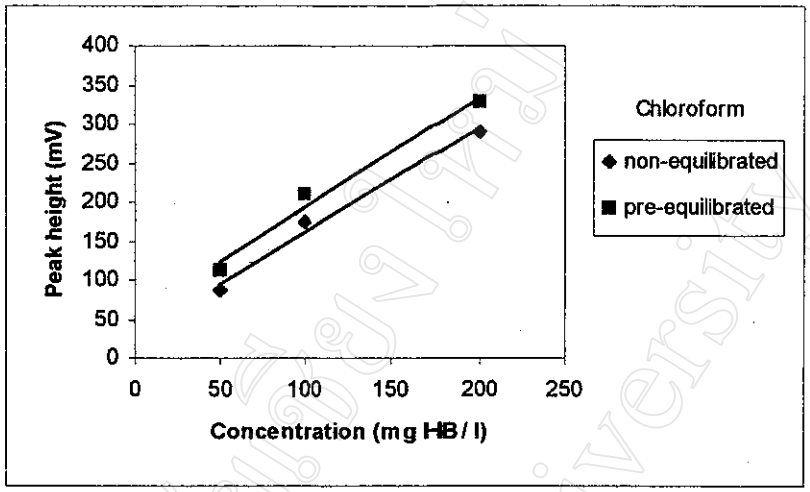

Figure 3.17 Effect of pre-equilibrated chloroform

3.2.2.2 Flow-rate of BB Reagent and Chloroform Stream

The results shown in Table 3.26 and Figure 3.18 indicated that the peak height was not quite different when the flow-rate of BB reagent stream and chloroform stream were used in the range 0.7-1.0 and 1.8-2.4 ml/min respectively. The flow-rate of 0.8 ml/min for BB reagent stream and 2.0 ml/min for chloroform stream were selected for further studies.

Table 3.26 Effect of flow-rate of BB reagent and chloroform streams

Flow rate (ml/min)		Peak height* (mV)			Calibration graph	r^2
BB reagent	Chloroform	HB Standard solution (mg HB/l)				
		50	100	200		
0.6	1.6	139	245	361	y = 1.434x + 81.0	0.9733
0.7	1.8	120	205	309	y = 1.229x + 68.0	0.9826
0.8	2.0	122	212	310	y = 1.214x + 73.0	0.9728
0.9	2.2	119	206	294	y = 1.126x + 75.0	0.9655
1.0	2.4	114	196	306	y = 1.254x + 59.0	0.9888

*Mean of triplicate injections

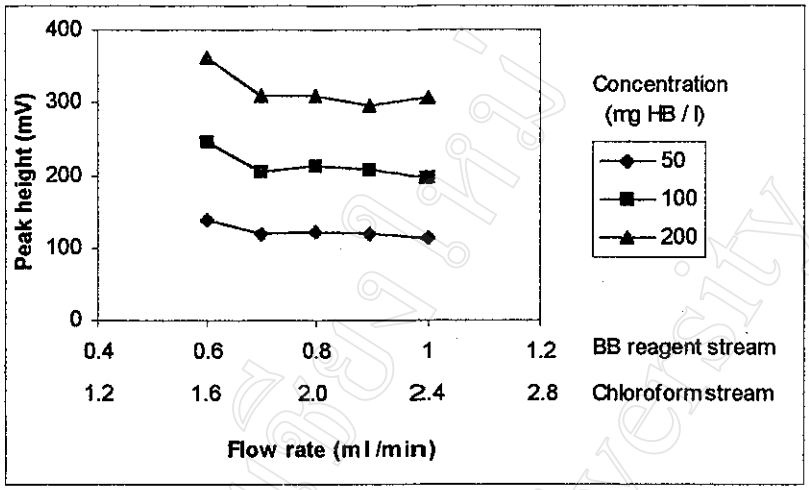

Figure 3.18 Effect of flow-rate of BB reagent and chloroform streams

3.2.2.3 Extraction Coil Length

The results are shown in Table 3.27 and Figure 3.19. It was found that the extraction coil length was increased the peak height increased. The negative peak occurred when using the extraction coil length of 100 cm. The extraction coil length of 50 cm was selected for further studies.

Table 3.27 Effect of extraction coil length

Extraction coil length (cm)	Peak height* (mV) HB standard solution (mg HB/l)			Calibration graph	r^2
	50	100	200		
none	42	73	105	y = 0.406x + 26.0	0.9676
50	121	205	324	y = 1.330x + 61.5	0.9918
100	154	255	364	y = 1.356x + 99.5	0.9720

*Mean of triplicate injections

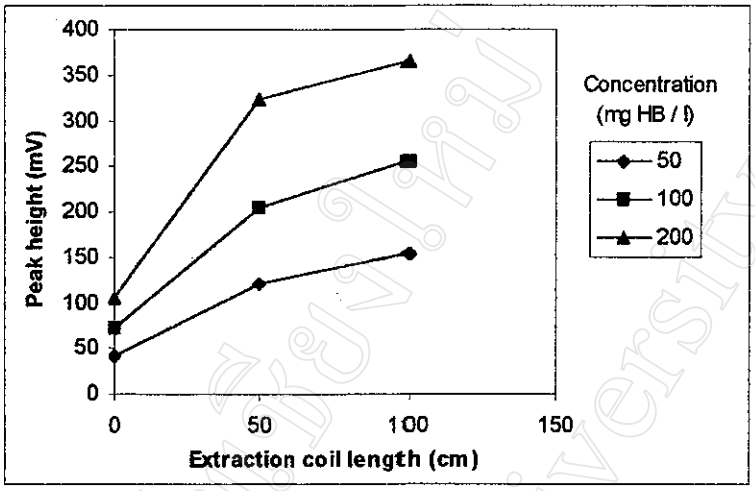

Figure 3.19 Effect of extraction coil length

3.2.2.4 Sample Volume

The results are displayed in Table 3.28 and Figure 3.20. It was found that the sample volume was increased the peak height increased. The negative peak occurred when using the sample volume of 80 µl. The sample volume of 50 µl was chosen for further studies.

Table 3.28 Effect of sample volume

Sample volume (µl)	Peak height* (mV) HB standard solution (mg HB/l)			Calibration graph	r^2
	50	100	200		
30	71	142	244	y = 1.134x + 20.0	0.9924
50	121	205	324	y = 1.330x + 61.5	0.9918
80	159	248	330	y = 1.094x + 118.0	0.9550

*Mean of triplicate injections

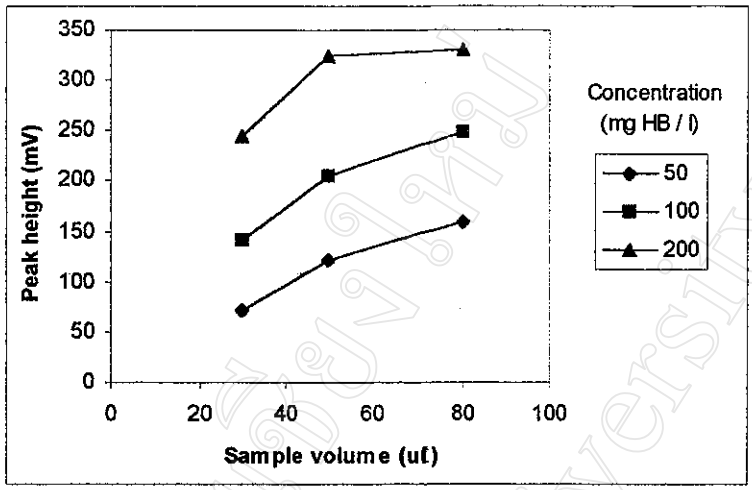

Figure 3.20 Effect of sample volume

3.2.2.5 pH of Bromothymol Blue Reagent Solution

The pH of bromothymol blue reagent solution was examined. Buffer solutions of disodium hydrogen phosphate/potassium dihydrogen phosphate (pH 7.0, 7.5 and 8.0), borate/sodium hydroxide (pH 9.3, 10.0 and 11.0) and glycine/sodium hydroxide (pH 12.0) were prepared as previously described [233]. 0.024% (w/v) BB in each buffer solution was prepared and three times of pre-extracted with chloroform. The results are shown in Table 3.29 and Figure 3.21. It was indicated that the peak height was not quite different when BB reagent was prepared in buffer solution of pH range 8.0-11.0. The BB in borate buffer solution pH 10.0 was selected.

Table 3.29 Effect of pH of bromothymol blue reagent solution

BB in buffer solution	pH	Peak height* (mV) HB standard solution (mg HB/l)			Calibration graph	r^2
		50	100	200		
Na_2HPO_4/KH_2PO_4	7.0	88	172	268	y = 1.166x + 40.0	0.9772
	7.5	120	222	328	y = 1.340x + 67.0	0.9683
	8.0	136	231	344	y = 1.350x + 79.5	0.9805
Borate/NaOH	9.3	164	271	382	y = 1.404x + 108.5	0.9681
	10.0	156	268	376	y = 1.411x + 102.0	0.9603
	11.0	152	250	366	y = 1.389x + 94.0	0.9801
Glycine/NaOH	12.0	68	116	203	y = 0.896x + 24.5	0.9994

*Mean of triplicate injections

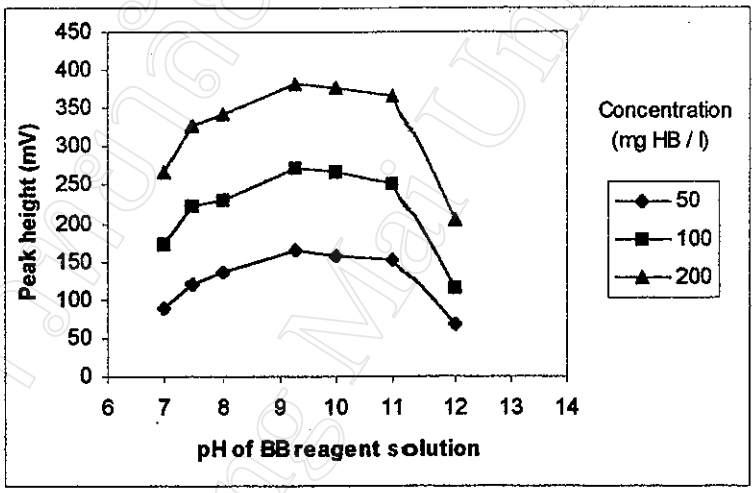

Figure 3.21 Effect of pH of bromothymol blue reagent solution

3.2.2.6 Bromothymol Blue Concentration

Various concentrations of bromothymol blue in borate buffer pH 10.0 were prepared and examined. The results shown in Table 3.30 and Figure 3.22 pointed out that the concentration of bromothymol blue was increased the peak height increased. The blue colour was attached on PTFE membrane when the concentration of bromothymol blue was used higher than 0.048% (w/v). This cause short lifetime of PTFE membrane. The bromothymol blue concentration of 0.048% (w/v) was selected.

Table 3.30 Effect of bromothymol blue concentration

Concentration of BB in borate buffer solution (% (w/v))	Peak height* (mV) HB standard solution (mg HB/l)					Calibration graph	r^2
	40	80	120	160	200		
0.006	88	121	148	178	188	y = 0.642x + 67.5	0.9754
0.012	118	206	260	300	348	y = 1.385x + 80.2	0.9744
0.024	158	266	336	386	418	y = 1.600x + 120.8	0.9500
0.048	135	266	368	460	548	y = 2.550x + 49.4	0.9931

*Mean of triplicate injections

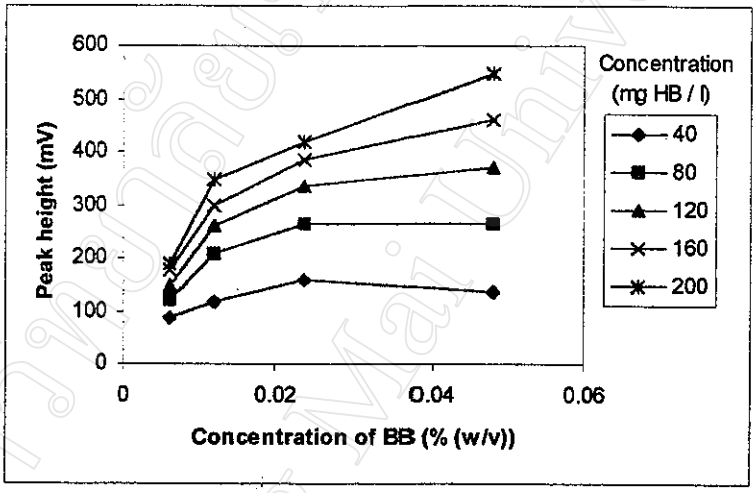

Figure 3.22 Effect of bromothymol blue concentration

3.2.3 Summary of the Optimum Conditions

The recommended FIA manifold with on-line solvent extraction shown in Figure 3.16 for the determination of hyoscine butylbromine has been optimized. The optimum conditions are summarized in Table 3.31.

Table 3.31 Optimum conditions

Parameter	Condition
Bromothymol blue reagent solution	0.048% (w/v) BB in borate buffer (pH 10.0)
Sample volume	50 µl
EC dimension	0.5 mm i.d. x 50 cm length
BC1 dimension	0.8 mm i.d. x 50 cm length
BC2 dimension	0.8 mm i.d. x 50 cm length
Flow-rate of BB reagent solution	0.8 ml/min
Flow-rate of chloroform	2.0 ml/min
Analytical wavelength	420 nm
Full scale range of recorder	1 V
Chart speed of recorder	5 mm/min

3.2.4 Calibration Graph and Detection Limit

The optimum conditions summarized in section 3.2.3 were used to perform a calibration graph. The results are displayed in Table 3.32, Figures 3.23 and 3.24. The detection limit ($3s_B$) [232] was also calculated as 18 mg HB/l.

Table 3.32 Peak height of standard HB solutions

HB Standard solution (mg HB/l)	Peak height* (mV)	Calibration graph
40	135	$y = 2.550x + 49.4$ $r^2 = 0.9931$
80	266	
120	368	
160	460	
200	548	

*Mean of triplicate injections

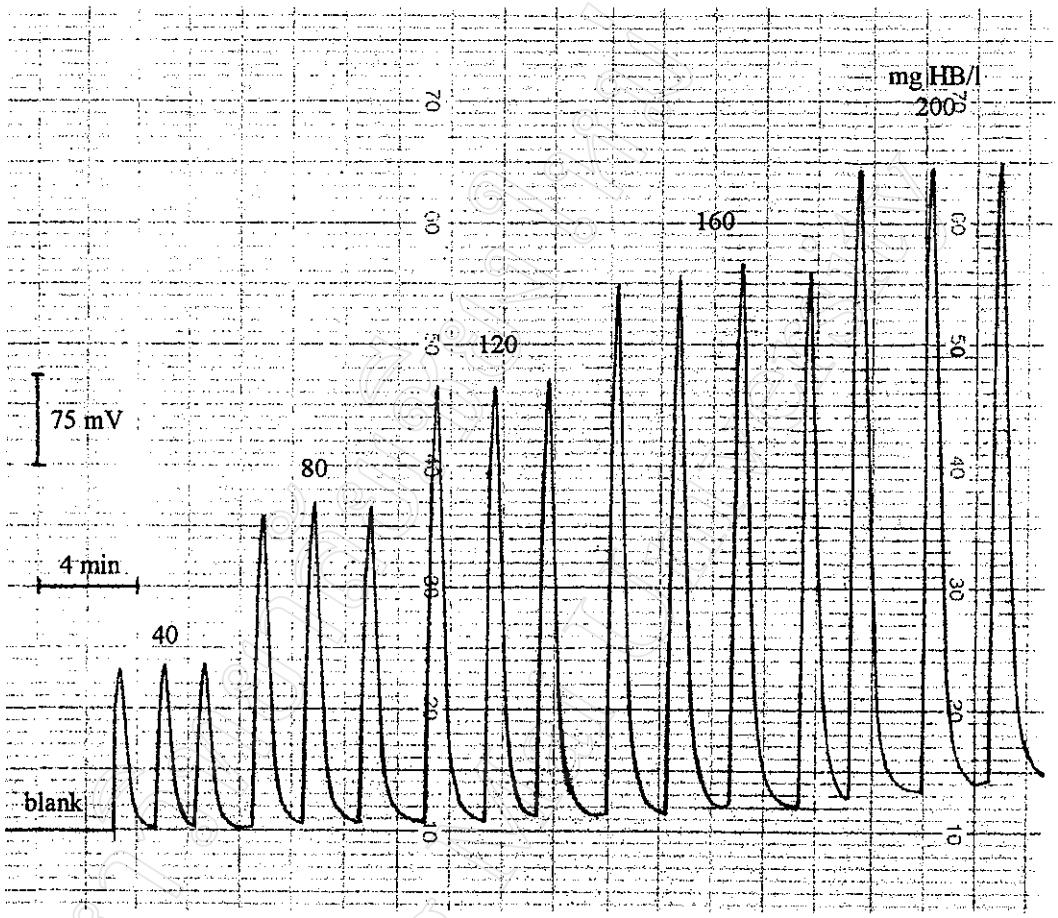

Figure 3.23 FIA-gram of HB standard solution

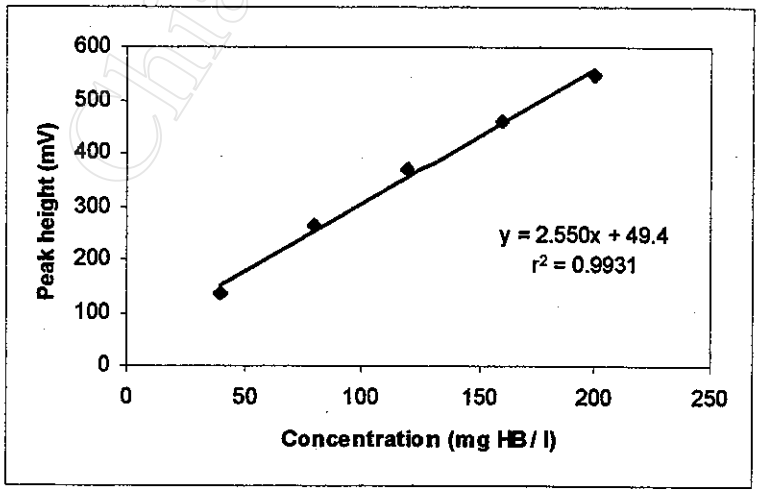

Figure 3.24 Calibration graph

3.2.5 Precision

The optimum conditions appeared in section 3.2.3 were used. The precision was determined by repeating injection of standard solution (120 mg HB/l) for 11 replicates. The results are shown in Table 3.33. The relative standard deviation (RSD) of 1.2% was obtained.

Table 3.33 Precision study

Standard HB Solution (mg HB/l)	Peak height (mV)	$\bar{X}$ (mV)	SD	%RSD
120	338, 340, 340, 335, 330, 335, 338, 330, 332, 330, 330	334	4	1.2

3.2.6 Interference Study

The effect of lactose was studied by adding lactose into hyoscine butylbromide standard solution (100 mg HB/l). The optimum conditions described in section 3.2.3 were used. Interference is considered to occur when causing peak height obtained lies outside the range $\bar{x} \pm 3SD$, where $\bar{x}$ is the response due to 100 mg HB/l alone. The results are shown in Table 3.34. It was indicated that the concentration of lactose up to 4000 mg/l did not interfere the determination of hyoscine butylbromide (100 mg HB/l).

Table 3.34 Interference study

Lactose added (mg/l)	Peak height (mV)	$\bar{x}$ (mV)	%Relative error
none	270, 265, 265, 265, 265, 262, 260, 262, 260, 262, 262	263*	-
1000	260, 262, 258	260	-1.1
2000	262, 262, 262	262	-0.4
4000	258, 260, 260	259	-1.5

*$\bar{x} \pm 3(SD) = 263 \pm 3(3) = 254\text{-}272$ $(n = 11)$

3.2.7 Determination of Hyoscine Butylbromide in Tablets

3.2.7.1 Sample Preparation [77]

Accurately weighed and powdered 20 tablets. Transferred a quantity of the powder equivalent to about 10 mg of hyoscine butylbromide to a 100 ml volumetric flask, added 50 ml of water, shook about ten minutes, and adjusted to volume with water, filter.

3.2.7.2 Determination

The optimum conditions displayed in section 3.2.3 were used to determine hyoscine butylbromide in 10 mg HB tablets. The results are shown in Table 3.35. A standard addition FIA method was also carried out. The calculated t-test value of the conventional FIA and standard addition FIA methods was 0.094. The critical value of t-test is 2.015 (5 degrees of freedom) at the confidence interval of 90% [232]. It was indicated that the results obtained by the conventional FIA and standard addition FIA methods were not significantly different with confidence interval of 90%.

Table 3.35 Determination of hyoscine butylbromide in tablets

Sample No.	Conc. of hyoscine butylbromide (mg HB/tablet)	
	Conventional FIA method	Standard addition FIA mehtod
1	9.4	-
2	7.2	-
3	3.1	-
4	2.9	-
5	8.9	8.8
6	5.0	4.8
7	4.3	4.1
8	8.4	8.3
9	4.7	5.6
10	7.8	7.6

3.2.8 Percentage Recovery

The percentage recoveries were determined by spiking various amounts of hyoscine butylbromide standard solutions into samples. The optimum conditions displayed in section 3.2.3 were used. The results are shown in Table 3.36. It was found that the percentage recoveries in range 80-100% were obtained by using the proposed FIA method involving on-line solvent extraction.

Table 3.36 Percentage recovery

Sample No.	HB standard solution added (mg HB/l)	HB found (mg HB/l)	% Recovery
5	0	53	-
	20	70	85
	40	89	90
	60	106	88
6	0	28	-
	20	48	100
	40	68	100
	60	87	98
7	0	24	-
	20	43	95
	40	59	87
	60	76	87
8	0	50	-
	20	69	95
	40	86	90
	60	100	83
9	0	34	-
	20	51	85
	40	66	80
	60	83	82
10	0	46	-
	20	63	85
	40	81	87
	60	98	87
			$\bar{x} = 89$

3.3 Flow Injection Spectrophotometric Determination of Yttrium with ArsenazoIII

1,8-Dihydroxynaphthalene-3,6-disulphonic acid-2,7-bis[(azo-2)-phenylarsonic acid] (ArsenazoIII) is one of the most sensitive reagents for yttrium. The chemical structure of arsenazoIII is shown in Figure 3.25.

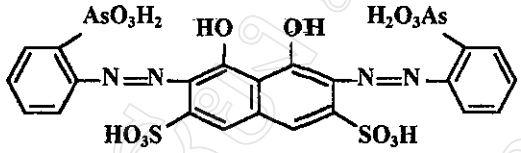

Figure 3.25 Chemical structure of arsenazoIII [100]

Yttrium(III) reacts with arsenazoIII to yield a blue-green 1:1 complex in the pH range 1.2-5.5, the molar absorptivity is 55000 l/mol.cm at 665 nm [106].

3.3.1 Preliminary Studies: Spectral Characteristics of the Yttrium-ArsenazoIII Complex

Buffer solutions of acetic acid/sodium acetate (pH 2.6-4.4), potassium hydrogen phthalate (KHP)/hydrochloric acid (pH 2.3-3.8), KHP/sodium hydroxide (pH 2.3-3.8), citrate/hydrochloric acid (pH 1.6-3.2), citrate/sodium hydroxide (pH 5.5-6.4), disodium hydrogen phosphate (Na_2HPO_4)/potassium dihydrogen phosphate (KH_2PO_4) (pH 6.7-7.2), borate/hydrochloric acid (pH 7.8, 8.8), glycine/sodium hydroxide (pH 8.5-12.3) and borate/sodium hydroxide (pH 9.9, 10.6) were prepared as previously described [233]. The absorption spectra of Y(III)-arsenazoIII complex were studied by varying pH of the solutions. The solutions containing 2.50 ml of 10 mg Y/l standard solution, 2.00 ml of 0.10% (w/v) arsenazoIII solution and 5.0 ml of each buffer solution were prepared and diluted to 50.0 ml with water. All electronic absorption spectra were recorded using a Shimadzu UV265 Spectrophotometer (Japan).

The spectra obtained from mixtures containing yttrium (5.6×10^{-5} M) and arsenazoIII (7.3×10^{-3} M) in various media are shown in Figure 3.26. In the acetic acid/acetate buffer (pH 2.6-4.4), the spectral characteristics were similar to those in the KHP/HCl buffer (pH 2.3-3.8); maximum absorption at 650 nm was observed, the same as previously reported [111].

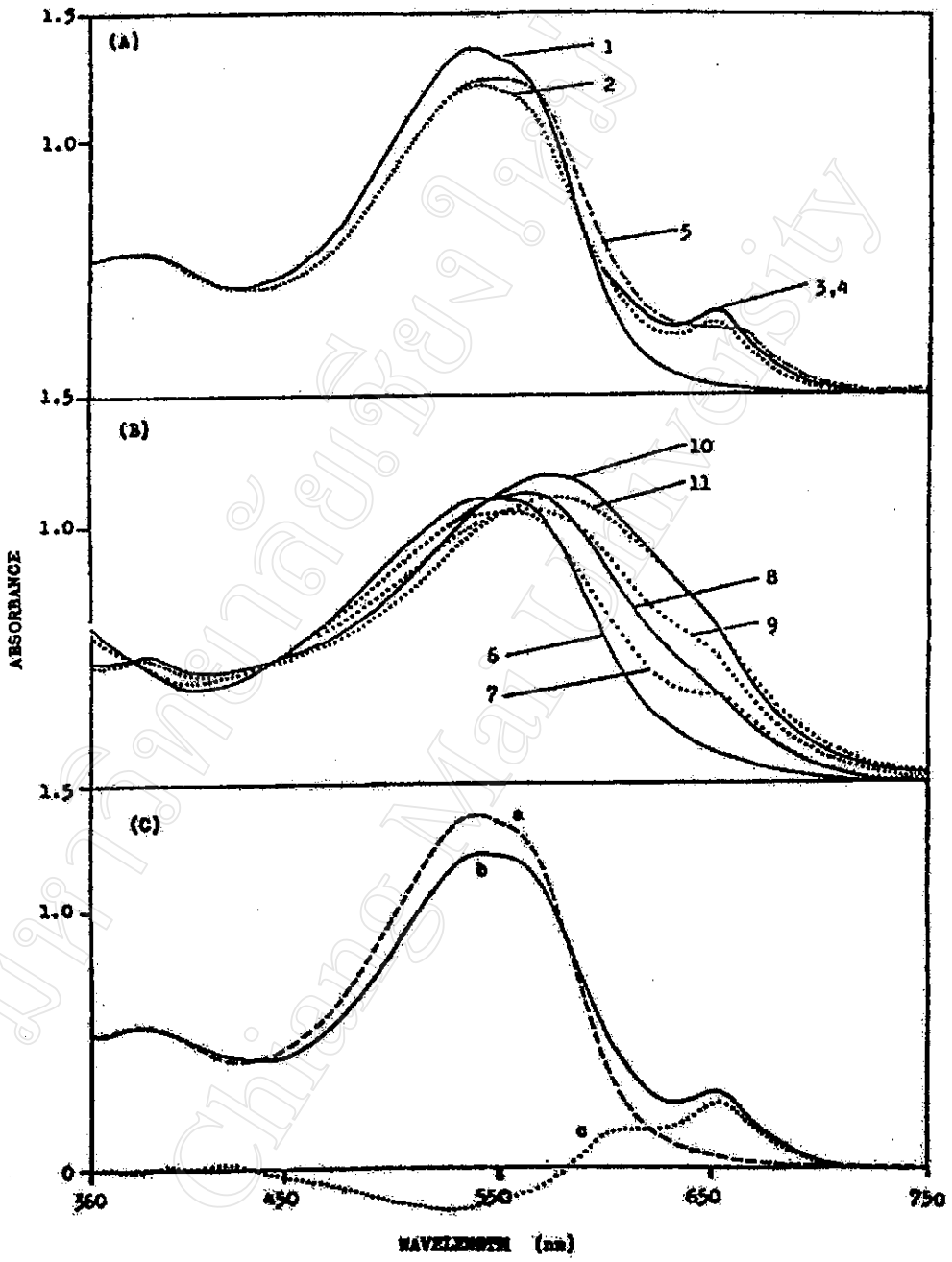

Figure 3.26 Spectra of Y-arsenazoIII complex in various media ($5.6x10^{-5}$ M Y; $1.3x10^{-3}$ M arsenazoIII): (A) 1, arsenazoIII, acetic acid/acetate pH 3.4; 2, complex, KCl/HCl pH 1.4; 3, complex, acetic acid/acetate pH 2.6; 4, complex, acetic acid/acetate pH 4.4; 5, complex, KHP/NaOH pH 5.8; (B) 6, arsenazoIII, borate/HCl pH 7.8; 7, complex, borate/HCl pH 7.8; 8, arsenazoIII, glycine/NaOH pH 9.7; 9, complex, glycine/NaOH pH 9.7; 10, arsenazoIII, glycine/NaOH pH 11.5; 11, complex, glycine/NaOH pH 11.5; (C) in acetic acid/acetate pH 3.9: a, reagent blank vs. H_2O; b, Y-arsenazoIII complex vs. H_2O; c, Y-arsenazoIII complex vs. reagent blank.

In the KHP/NaOH (pH 4.5-5.8) or Na_2HPO_4/KH_2PO_4 (pH 5.6) buffers, the molar absorptivities observed were less than those in the acetic acid/acetate or KHP/HCl buffers. Reagent blanks were observed to be higher in the former conditions. The buffers containing citrate shown the effects on absorption spectra; this may be due to the competitive forming of a complex of citrate and yttrium. Effects of the buffers Na_2HPO_4/KH_2PO_4 (pH 6.7-7.2), borate/HCl (pH 7.8, 8.8), glycine/NaOH (pH 8.5-12.3), and borate/NaOH (pH 9.9, 10.6) were found to be more pronounced. This could be due to the possibility of binding of the anionic species such as phosphate or borate and the hydrolysis of yttrium in media with higher pH values. From the results, the most appropriate pH range for colour formation was pH 2.3-5.5, with an acetic acid/acetate or KHP/HCl buffer.

3.3.2 Manifold and Procedure

The FIA manifold for the determination of yttrium using arsenazoIII was introduced by modifying the QuikChem 4200 (Lachat Instrument, Milwaukee, WI, USA).The manifold is shown in Figure 3.27.

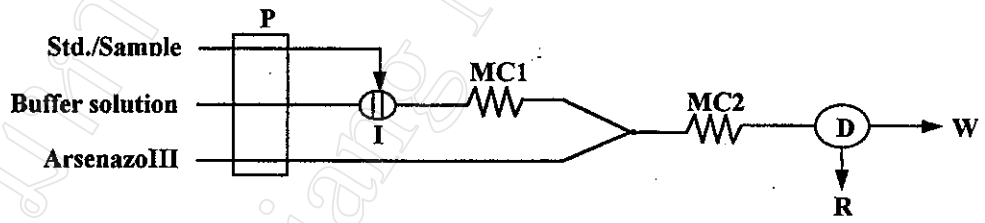

Figure 3.27 FIA manifold for the determination of yttrium using arsenazoIII; P = peristaltic pump; I = injection valve; MC = mixing coils; D = spectrophotometer; R = chart recorder; W = waste

A standard or sample is injected via a sample loop into a stream of buffer solution, which passes through a mixing coil (MC1) before merging with the reagent stream of arsenazoIII. After passing through a second mixing coil (MC2), the coloured complex that is produced in the stream is continuously monitored at 650 nm.

3.3.3 Optimization

The manifold illustrated in Figure 3.27 was used. Preliminary conditions are shown in Table 3.37 for the optimization studied by varying one parameter while the others were kept constant.

Table 3.37 Preliminary conditions

Parameter	Condition
Buffer solution	0.10 M acetic acid/acetate buffer (pH 3.5)
ArsenazoIII	0.010% (w/v) arsenazoIII
Sample volume	150 µl
MC1 dimension	0.8 mm i.d. x 50 cm length
MC2 dimension	0.8 mm i.d. x 50 cm length
Flow-rate of buffer solution	1.4 ml/min
Flow-rate of arsenazoIII	1.4 ml/min
Analytical wavelength	650 nm
Full scale range of recorder	1.0 V
Chart speed of recorder	5 mm/min

3.3.3.1 ArsenazoIII Concentration

The results are shown in Table 3.38 and Figure 3.28. It was found that the highest peak height obtained when the arsenazoIII concentration of 0.0010% (w/v) was used. The arsenazoIII concentration of 0.0010% (w/v) was selected for further studies.

Table 3.38 Effect of arsenazoIII concentration

Standard solution (mg Y/l)	**Peak height* (mV)**		
	Concentration of arsenazoIII (% (w/v))		
	0.0001	**0.0010**	**0.0100**
0.20	89	117	66
0.40	105	245	150
0.60	110	376	182
0.80	114	487	292
1.00	117	615	383
Calibration graph	$y = 32.5x + 87.5$	$y = 619.0x - 3.4$	$y = 388.0x - 18.2$
r^2	0.8693	0.9994	0.9765

*Mean of triplicate injections

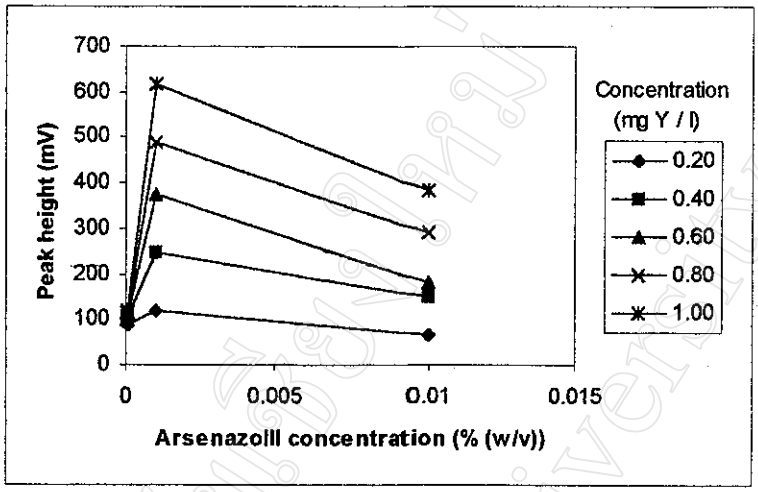

Figure 3.28 Effect of arsenazoIII concentration

3.3.3.2 pH of Acetic Acid/Acetate Buffer Solution

The results are displayed in Table 3.39 and Figure 3.29. It was indicated that the peak height was not quite different when the pH of acetic acid/acetate buffer solution was used in the range 3.5-4.5. The acetic acid/acetate buffer solution pH 4.0 was chosen for further studies.

Table 3.39 Effect of pH of acetic acid/acetate buffer solution

pH	Peak height* (mV) Standard solution (mg Y/l)			Calibration graph	r^2
	0.20	0.40	0.60		
3.0	137	280	420	y = 707.5x – 4.0	1.0000
3.5	117	245	376	y = 647.5x – 13.0	1.0000
4.0	120	253	388	y = 670.0x – 14.3	1.0000
4.5	126	250	382	y = 640.0x – 3.3	0.9997

*Mean of triplicate injections

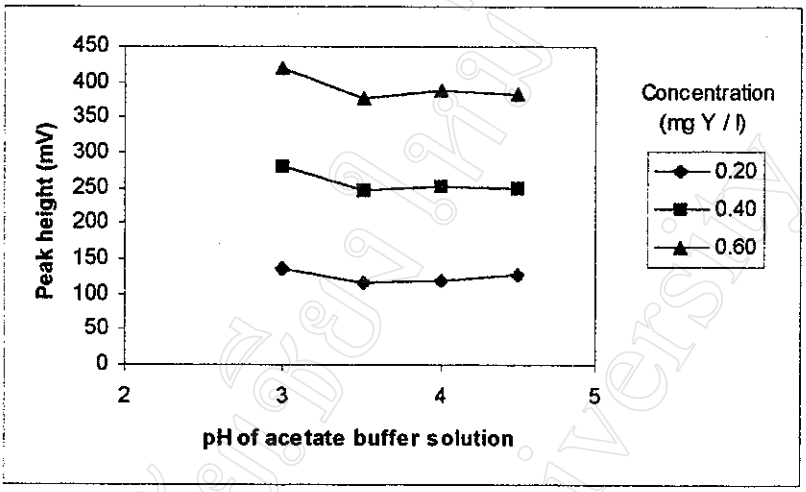

Figure 3.29 Effect of pH of acetic acid/acetate buffer solution

3.3.3.3 Mixing Coil 1 Length

The results shown in Table 3.40 and Figure 3.30 indicated that the MC1 length was increased the peak height decreased. The reproducible peak height was not obtained when the MC1 length of 12 cm was used. The MC1 length of 50 cm was selected for the further studies.

Table 3.40 Effect of MC1 length

Standard solution (mg Y/l)	**Peak height* (mV)**		
	Mixing coil 1 length (cm)		
	12	**50**	**100**
0.20	142	112	76
0.40	308	270	172
0.60	479	418	272
0.80	670	564	406
1.00	815	696	495
Calibration graph	y = 854.0x - 29.6	y = 731.0x – 26.6	y = 536.0x – 37.4
r^2	0.9987	0.9990	0.9962

*Mean of triplicate injections

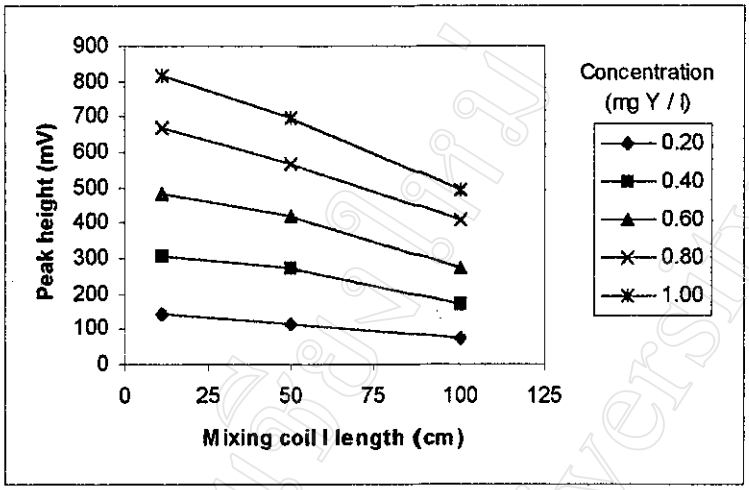

Figure 3.30 Effect of MC1 length

3.3.3.4 Mixing Coil 2 Length

The results displayed in Table 3.41 and Figure 3.31 pointed out that the MC2 length was increased the peak height decreased. The reproducible peak height was not obtained when the MC2 length of 12 cm was used. The MC2 length of 50 cm was chosen for next studies.

Table 3.41 Effect of MC2 length

Standard solution (mg Y/l)	**Peak height* (mV)**		
	Mixing coil 2 length (cm)		
	12	**50**	**100**
0.20	124	112	83
0.40	284	270	188
0.60	430	418	315
0.80	591	564	428
1.00	700	696	539
Calibration graph	y = 729.5x - 11.9	y = 731.0x – 26.6	y = 576.0x – 35.0
r^2	0.9962	0.9990	0.9993

*Mean of triplicate injections

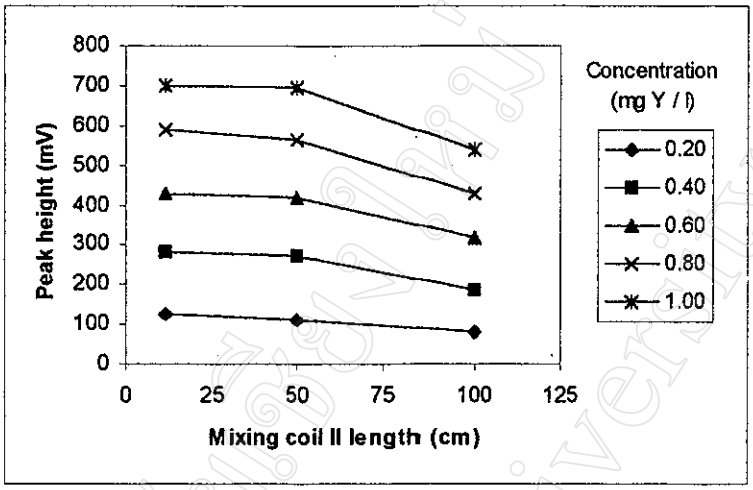

Figure 3.31 Effect of MC2 length

3.3.3.5 Sample Volume

The results shown in Table 3.42 and Figure 3.32 indicated that the sample volume was increased the peak height increased. The reproducible peak height was not obtained when the sample volume of 200 µl was used. The sample volume of 150 µl was selected.

Table 3.42 Effect of sample volume

Standard solution (mg Y/l)	**Peak height* (mV)**		
	Sample volume (µl)		
	120	**150**	**200**
0.20	82	112	148
0.40	175	270	328
0.60	286	418	510
0.80	406	564	693
1.00	523	696	844
Calibration graph	y = 556.5x - 39.5	y = 731.0x – 26.6	y = 878.5x – 22.5
r^2	0.9978	0.9990	0.9988

*Mean of triplicate injections

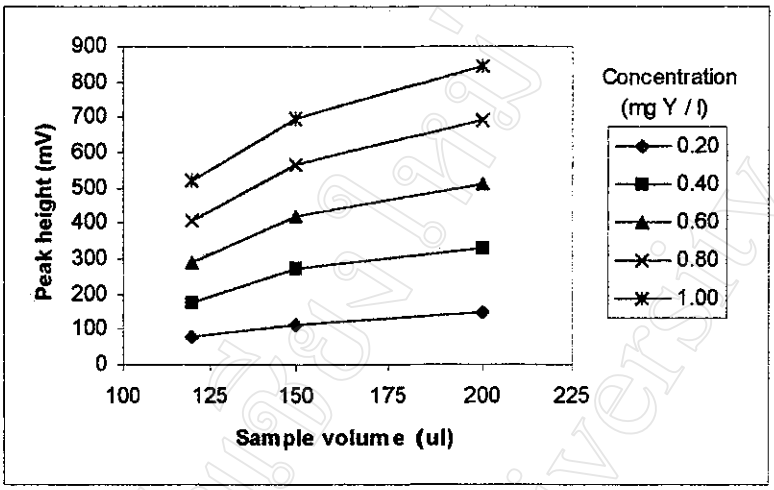

Figure 3.32 Effect of sample volume

3.3.3.6 Flow-rate of Buffer Solution and ArsenazoIII Streams

The results are displayed in Table 3.43 and Figure 3.33. It was found that the flow-rate was increased the peak height increased when the flow-rate was changed from 0.8 to 1.4 ml/min. The rather constant peak height was obtained when the flow-rate was used in the range 1.4-1.9 ml/min. The flow-rate of 1.4 ml/min was selected for both buffer solution and arsenazoIII streams.

Table 3.43 Effect of flow-rate of buffer solution and arsenazoIII streams

Flow rate (ml/min)		Peak height* (mV)					Calibration graph	r^2
Buffer solution	ArsenazoIII	Standard solution (mg Y/l)						
		0.20	0.40	0.60	0.80	1.00		
0.8	0.8	96	227	349	502	619	y = 660.5x – 37.7	0.9986
1.4	1.4	112	270	418	564	696	y = 731.0x – 26.6	0.9990
1.9	1.9	114	262	418	568	699	y = 738.0x – 30.6	0.9991

*Mean of triplicate injections

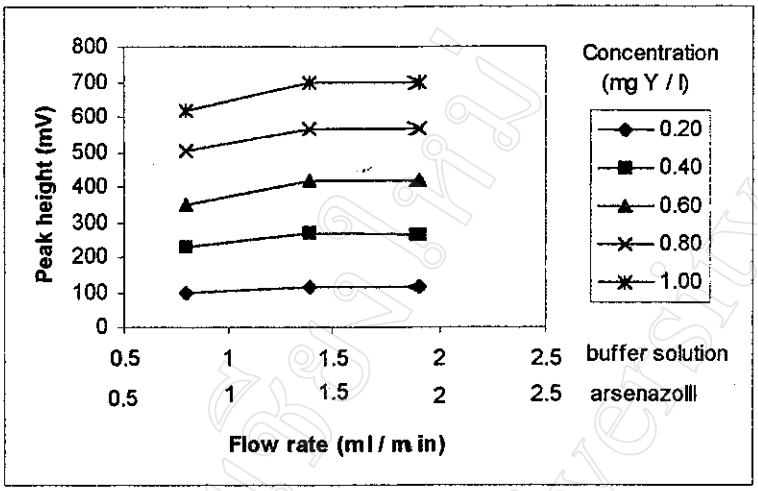

Figure 3.33 Effect of flow-rate of buffer solution and arsenazoIII streams

3.3.3.7 Buffer Solutions

The different buffer solutions were also studied. A buffer (pH 4.0; 0.10 M) of either acetic acid/acetate or KHP/HCl can be used. The 0.10 M acetic acid/acetate buffer solution (pH 4.0) was selected for the further studies. The results were as follows:

3.3.3.7.1 Citrate Buffer

Citrate buffer solutions (0.002 M, 0.010 M and 0.100 M; pH 3.0, 4.0 and 5.0) were prepared as previously described [233]. The effect of citrate buffer solution was studied. The results are shown in Table 3.44 and Figure 3.34. It was observed that as the concentration of citrate increased, the peaks decreased. For pH 3.0, a linear calibration graph was obtained when using the 0.002 M citrate buffer. With 0.010 M citrate buffer, a linear calibration with a lower slope than with 0.002 M citrate buffer was obtained. With the 0.100 M citrate buffer, the same height of the peaks was obtained for all the standards used. Similar trends were observed for citrate buffers of both pH 4.0 and 5.0. This is because citrate forms a stable complex with yttrium, which prevents it from reacting with the arsenazoIII reagent.

Table 3.44 Effect of citrate buffer

Citrate buffer solution		Peak height* (mV) Standard solution (mg Y/l)					Calibration graph	r^2
pH	Conc. (M)	0.20	0.40	0.60	0.80	1.00		
3.0	0.002	83	174	280	414	486	y = 523.0x – 26.4	0.9932
	0.010	49	97	152	209	258	y = 265.0x – 6.0	0.9991
	0.100	44	47	49	52	56	y = 14.5x + 40.9	0.9871
4.0	0.002	60	141	234	343	410	y = 451.0x – 33.0	0.9956
	0.010	12	26	44	79	96	y = 110.5x – 14.9	0.9762
	0.100	23	23	22	24	25	-	-
5.0	0.100	18	16	17	18	18	-	-

*Mean of triplicate injections

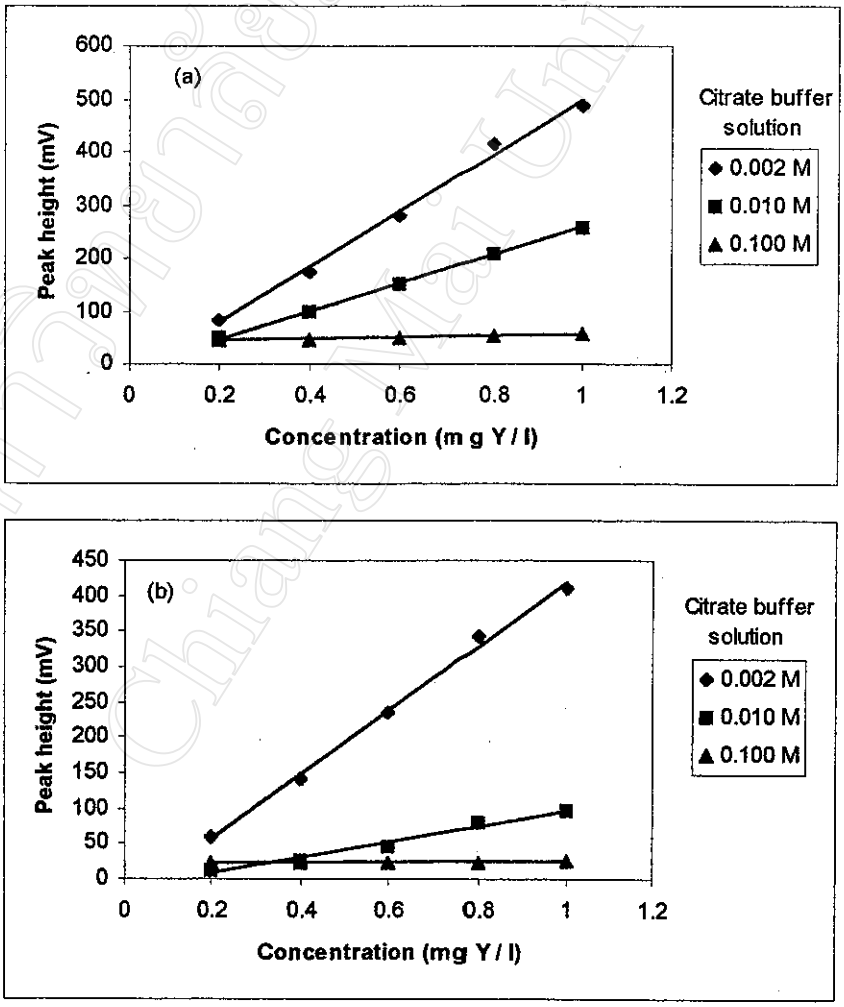

Figure 3.34 Effect of citrate buffer
(a) pH 3.0; (b) pH 4.0

3.3.3.7.2 Acetic Acid/Acetate Buffer

The acetic acid/acetate buffer (pH 4.0) has been previously chosen in section 3.3.3.2. The effect of concentration of acetic acid/acetate buffer was studied in this section. The results are displayed in Table 3.45 and Figure 3.35. The higher response of the blank occurred when using the 1.00 M acetic acid/acetate buffer. The linear calibration graph was obtained when using either 0.10 M or 1.00 M acetic acid/acetate buffer (pH 4.0). The 0.10 M acetic acid/acetate buffer solution (pH 4.0) was selected.

Table 3.45 Effect of concentration of acetic acid/acetate buffer (pH 4.0)

Standard solution (mg Y/l)	Concentration of acetic acid/acetate buffer (pH 4.0)			
	0.10 M		1.00 M	
	Peak height* (mV)	Corrected for blank (mV)	Peak height* (mV)	Corrected for blank (mV)
Blank	0	-	32	-
0.20	92	92	103	71
0.40	250	250	224	192
0.60	386	386	382	350
0.80	535	535	505	473
1.00	650	650	615	583
Calibration graph	y = 700.5x – 37.7		y = 652.5x – 57.7	
r^2	0.9975		0.9964	

*Mean of triplicate injections

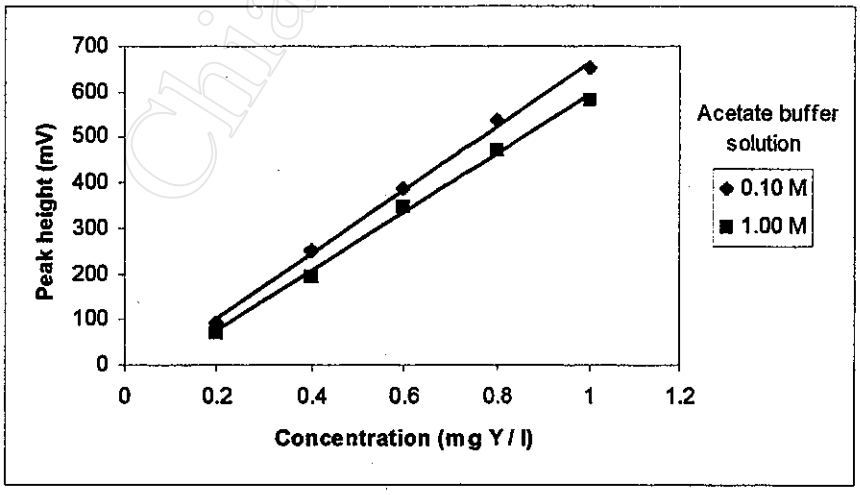

Figure 3.35 Effect of concentration of acetic acid/acetate buffer (pH 4.0)

3.3.3.7.3 KHP/HCl Buffer

The KHP/HCl buffer solution (pH 4.0) was also tried. The effect of concentration of KHP/HCl buffer was studied. The results are shown in Table 3.46 and Figure 3.36. The higher response of the blank was obtained when using the 0.50 M KHP/HCl buffer. The calibration graph of 0.10 M KHP/HCl buffer produced a higher slope than 0.50 M buffer. The 0.10 M KHP/HCl buffer solution (pH 4.0) can be used.

Table 3.46 Effect of KHP/HCl buffer

Standard solution (mg Y/l)	Concentration of KHP/HCl buffer (pH 4.0)			
	0.10 M		0.50 M	
	Peak height* (mV)	Corrected for blank (mV)	Peak height* (mV)	Corrected for blank (mV)
Blank	7	-	69	-
0.20	120	113	137	68
0.50	312	305	299	230
0.80	520	513	418	349
1.00	616	609	535	466
Calibration graph	$y = 631.3x - 9.6$		$y = 484.8x - 24.8$	
r^2	0.9967		0.9953	

*Mean of triplicate injections

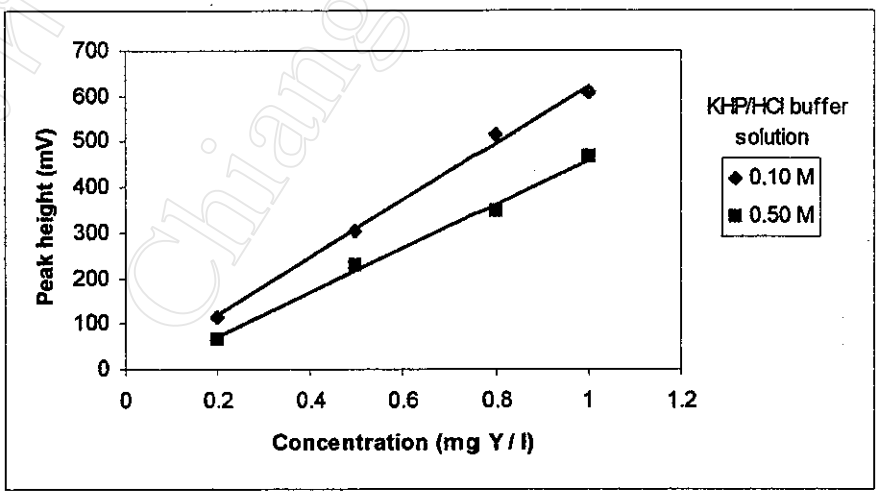

Figure 3.36 Effect of KHP/HCl buffer

3.3.3.8 pH of Standard Solution

A standard, adjusted to various pH values by using HCl and/or NaOH solutions, was injected into the buffer carrier stream (pH 4.0) of the FI system. 0.10 M of acetic acid/acetate buffer and KHP/HCl buffer were used. The results are shown in Table 3.47 and Figure 3.37. Practically constant peak heights could be maintained for the pH range of 3.0-4.0 for both 0.10 M buffers of acetic acid/acetate and of KHP/HCl.

Table 3.47 Effect of pH of standard solution

Standard solution (mg Y/l)	pH of standard	Peak height* (mV)					
		0.10 M acetic acid/acetate buffer pH 4.0			0.10 M KHP/HCl buffer pH 4.0		
		Blank	Peak height	Corrected for blank	Blank	Peak height	Corrected for blank
0.05	1.6	-	-	-	1	13	12
	3.2	-	-	-	10	24	14
	5.3	-	-	-	7	19	12
	5.6	-	-	-	7	10	3
	8.4	-	-	-	7	16	9
	11.8	-	-	-	40	62	22
0.10	1.6	-	-	-	1	32	31
	3.2	-	-	-	10	46	36
	4.9	-	-	-	7	37	30
	5.4	-	-	-	7	31	24
	7.1	-	-	-	7	28	21
	11.8	-	-	-	40	124	84
0.50	1.6	0	112	112	0	143	143
	3.2	5	307	302	16	290	274
	4.2	2	307	305	7	315	308
	6.2	2	236	234	7	236	229
	9.8	2	30	28	7	237	230
	10.3	2	48	46	7	228	221
	11.4	14	34	20	12	162	150
	11.8	14	38	24	28	47	19
1.00	1.6	0	236	236	0	291	291
	3.1	5	659	654	16	590	574
	4.0	2	672	670	7	602	595
	6.5	2	728	726	7	661	654
	9.7	2	200	198	7	442	435
	10.3	2	39	37	7	434	427
	11.4	14	30	16	12	311	299
	11.8	14	47	33	28	171	143

*Mean of triplicate injections

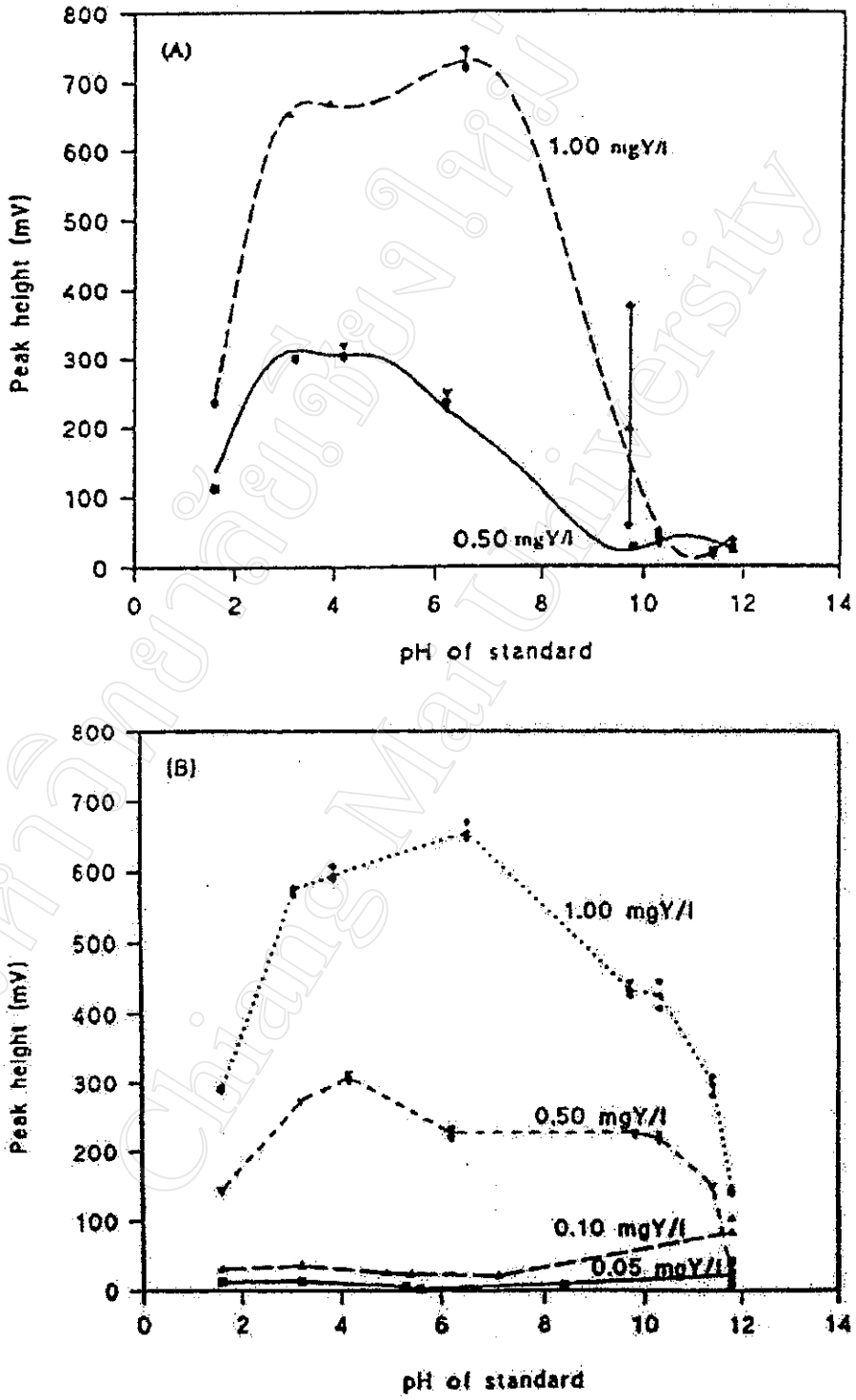

Figure 3.37 Effect of pH of standard solution when using buffer (0.10 M; pH 4.0): (A) acetic acid/acetate and (B) KHP/HCl

3.3.4 Summary of the Optimum Conditions

The recommended FIA manifold shown in Figure 3.27 for the determination of yttrium using arsenazoIII has been optimized. The optimum conditions are summarized in Table 3.48.

Table 3.48 Optimum conditions

Parameter	Condition
Buffer solution	0.10 M acetic acid/acetate buffer (pH 4.0)
ArsenazoIII	0.010% (w/v) arsenazoIII
Sample volume	150 µl
MC1 dimension	0.8 mm i.d. x 50 cm length
MC2 dimension	0.8 mm i.d. x 50 cm length
Flow-rate of buffer solution	1.4 ml/min
Flow-rate of arsenazoIII	1.4 ml/min
Analytical wavelength	650 nm
Full scale range of recorder	1.0 V
Chart speed of recorder	5 mm/min

3.3.5 Calibration Graph and Detection Limit

The optimum conditions summarized in section 3.3.4 were used to perform a calibration graph and to estimate the detection limit. The results are displayed in Table 3.49, Figures 3.38 and 3.39. The detection limit ($3S_B$) [232] was calculated as 0.02 mg Y/l.

Table 3.49 Peak height of yttrium standard solutions

Standard solution (mg Y/l)	Peak height* (mV)	Calibration graph
0.10	44	$y = 710.3x - 30.0$ $r^2 = 0.9995$
0.20	117	
0.40	246	
0.60	391	
0.80	540	
1.00	684	

*Mean of triplicate injections

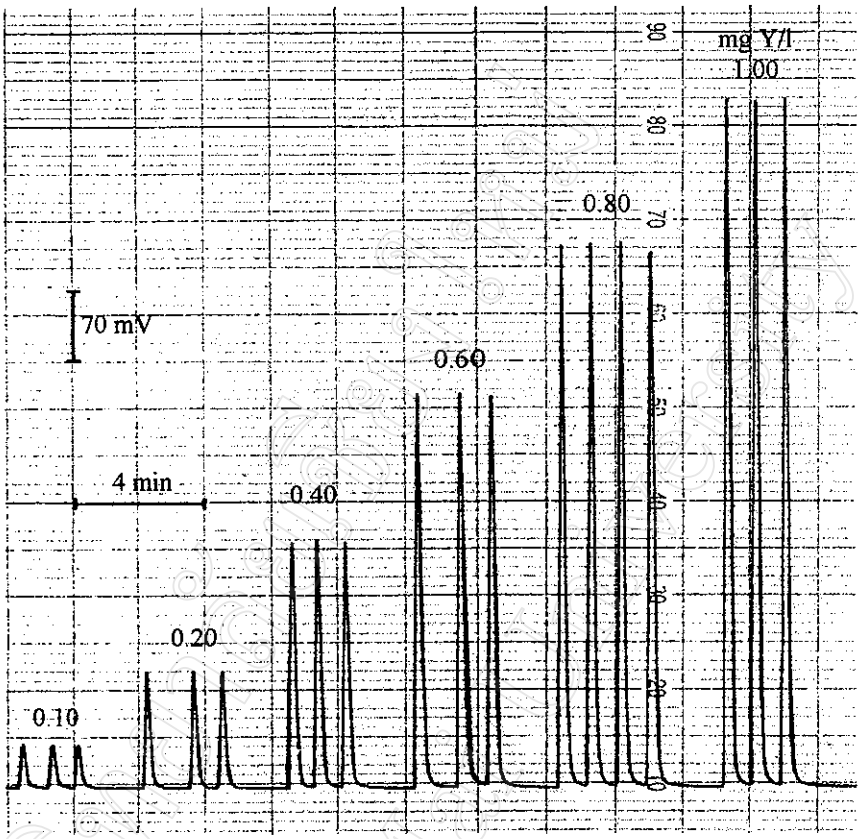

Figure 3.38 FIA-gram of yttrium standard solutions

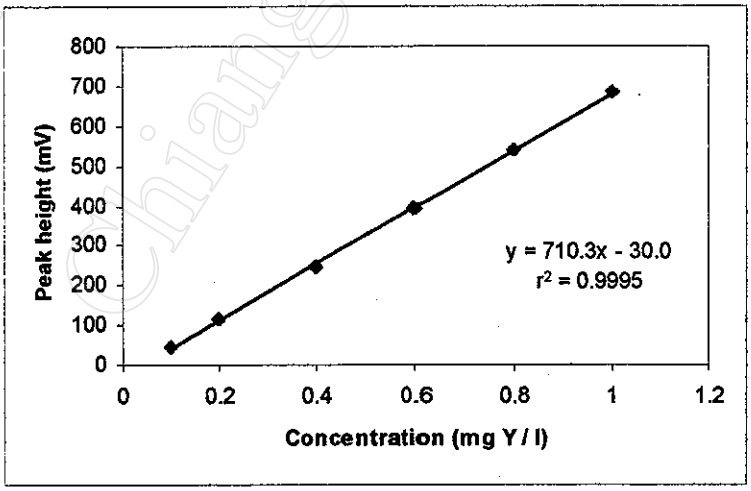

Figure 3.39 Calibration graph

3.3.6 Precision

The optimum conditions summarized in section 3.3.4 were used. The precision was estimated by repeating injection of standard solution (0.40 mg Y/l) for 11 replicates. The results are shown in Table 3.50. The relative standard deviation of 0.8% was obtained.

Table 3.50 Precision study

Standard Solution (mg Y/l)	Peak height (mV)	$\bar{x}$ (mV)	SD	%RSD
0.40	245, 245, 248, 250, 250, 252, 250, 252, 250, 250, 250	249	2	0.8

3.3.7 Interference Study

Applying the optimum conditions, solutions containing 0.10 mg Y/l and the respective ion with appropriate amounts were studied. The concentration at which an ion would interfere is determined when a relative error of 10% of the peak height of the original solution of 0.10 mg Y/l is obtained. The results are listed in Table 3.51 and summarized in Table 3.52

Table 3.51 Effect of interfering ions

Ion added	Concentrations (%) of ion in 0.10 mg Y/l	Peak height* (mV)	% Relative error
none	-	46	-
Zr(IV)	1	45	- 2.2
	4	70	+ 5.2
Cd(II)	1	50	+ 8.7
	4	56	+ 22
Zn(II)	1	49	+ 6.5
	4	61	+ 33
La(III)	1	44	- 4.3
	4	52	+ 13
U(VI)	1	48	+ 4.3
	4	44	- 4.3
	10	36	- 22
Cu(II)	1	45	- 2.2
	4	42	- 8.7
	10	38	- 17

*Mean of triplicate injections

Table 3.51 Continue...

Ion added	Concentrations (%) of ion in 0.10 mg Y/l	Peak height* (mV)	% Relative error
Mn(II)	1	48	+ 4.3
	4	49	+ 6.5
	10	52	+ 13
Ti(III)	1	50	+ 8.7
	4	49	+ 6.5
	10	53	+ 15
Mg	1	48	+ 4.3
	4	47	+ 2.2
	10	52	+ 13
Th(IV)	1	46	0
	4	48	+ 4.3
	10	52	+ 13
Ba	1	47	+ 2.2
	4	45	.- 2.2
	10	53	+ 15
Ca	1	44	- 4.3
	4	49	+ 6.5
	10	49	+ 6.5
Fe(III)	1	44	- 4.3
	4	45	- 2.2
	10	42	- 8.7

*Mean of triplicate injections

Table 3.52 Summarized results for the effect of interfering ions

Maximum concentrations (%) of ion in 0.10 mg Y/l*	Ions
1	Zr(IV), Cd(II), Zn(II), La(III)
4	U(VI), Cu(II), Mn(II), Ti(III), Mg, Th(IV), Ba
10	Ca, Fe(III)

* Maximum concentration of an ion contained in 0.10 mg Y/l yielding a relative error of $< \pm 10\%$ of the peak height of the solution of 0.10 mg Y/l alone

3.3.8 Determination of Yttrium in Samples

The flow-injection procedure with the optimum conditions summarized in section 3.3.4 was applied to determine yttrium contents in a digest of a reference material, IGS36 (Institute of Geological Science, London, UK). The digestion was performed with HNO_3, HF, and $HClO_4$,

followed by HCl and H_3BO_4 [234] and with in a reference solution, SPEX CALMIX-4 (SPEX Industries, Inc. NJ., USA).

The procedure was also applied to leachates of some mineral samples collected in Thailand. The samples (0.1 or 0.2 g) were leached with conc. H_2SO_4 (5 ml) at 250 °C for 2 hours. After filtering, the filtrates were adjusted to 100 ml with water. Appropriated dilutions with 0.10 M acetic acid/acetate buffer (pH 4.0) were made before injection into the FIA system. Yttrium contents were obtained via a calibration graph.

The results are shown in Table 3.53. The ICP-AES was also used to determine yttrium contents in these samples. The differences between the means obtained from the proposed FIA method and the reference method were evaluated by t-test. The calculated t-test value of the proposed FIA and ICP-AES methods was 1.456. The critical value of t-test is 1.895 (7 degrees of freedom) at the confidence interval of 90% [232]. It was pointed out that the results obtained by the recommended method were not significantly different from those obtained by the ICP-AES method with confidence interval of 90%.

Table 3.53 Determination of yttrium contents in samples

Sample	Y content (% (w/v))	
	FIA	**ICP-AES[a]**
IGS 36	0.99	1.12
SPEX CALMIX-4	0.01	0.01[b]
Y1	0.12	0.13
Y2	0.06	0.07
Y3	0.09	0.10
Y4	0.03	0.04
Y5	0.03	0.03
Y6	0.07	0.08

[a] Analyzed by the Central Lab of the Department of Mineral Resources, Bangkok, Thailand

[b] Certified value: 100 ± 10 mg Y/l

3.4 Determination of Cobalt(II) and Manganese(II) in Reused Catalyst by Spectrophotometric FIA

In the catalytic process for terephthalic acid preparation from p-xylene, which involves the air oxidation of p-xylene in a liquid acetic acid solution, the catalyst system is made of bromides of heavy metals and salts of cobalt and manganese [230, 231]. In order to utilize this expensive catalyst effectively, it is important to reuse. So it is necessary to determine Co(II) and Mn(II) contents in liquid residue before reuse of this catalyst.

3.4.1 Compatible Solvent

Preparation of the stock standard solutions of Co(II) and Mn(II) in mixed solvent (70:22:8 by volume of glacial acetic acid: xylene: deionized water) have been made in order that the components in this solution were similar to the sample system. 50% (v/v) Isopropanol solution was selected to dilute the samples and the stock standard solutions as optimum compatible solvent so the experiments can easily proceed in aqueous system.

3.4.2 Flow-Injection Spectrophotometric Determination of Co(II) with PAR

4-(2-Pyridylazo)resorcinol, given the acronym PAR, is one of the most sensitive reagents for cobalt. The chemical structure of PAR is shown in Figure 3.40.

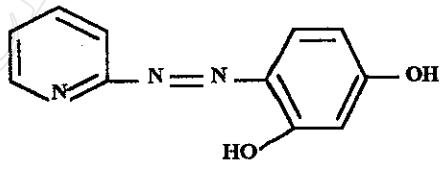

Figure 3.40 Chemical structure of PAR [235]

Co(II) and PAR form a water-soluble, red-coloured complex with an absorbance maximum at 510 nm. The molar absorptivity of the Co(II)-PAR complex (pH 8.25) is 5.6×10^4 l/mol.cm at 510 nm [235].

3.4.2.1 Preliminary Studies: Spectral Characteristics of Co(II)-PAR Complex

The absorption spectra of Co(II)-PAR complex were studied by varying pH of the solutions. The solutions containing 5.00 ml of standard solution (6.0 mg Co/l) and 5.00 ml of 0.030% (w/v) PAR were prepared and adjusted to require pH value using conc. HNO_3 before diluted to 50.0 ml with water. The solutions containing manganese(II) standard solution instead of cobalt(II) and blank solutions were also prepared. All absorption spectra were recorded using a HITACHI U-2000 Spectrophotometer (Japan). The recorded absorption spectra are displayed in Figure 3.41. It was indicated that the optimum pH value should be selected at pH 6.0 (λ_{max} = 520 nm) for the determination of Co (II) with PAR, because Mn(II) did not interfere and sensitivity was higher than at pH 4.0.

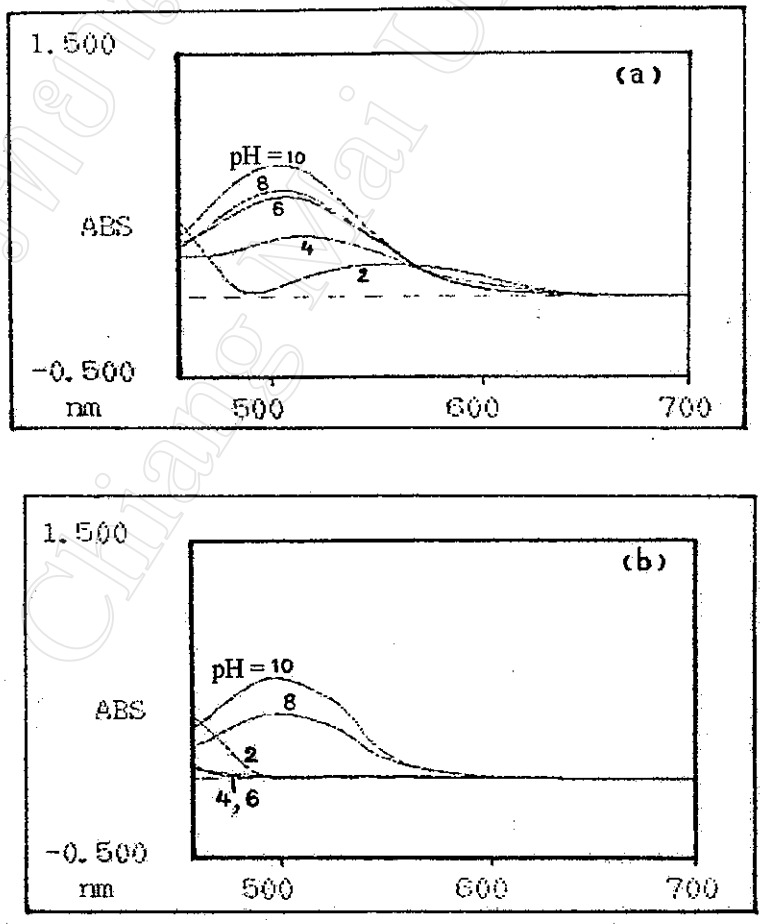

Figure 3.41 Absorption spectra at various pH
(a) Co(II)-PAR complex versus blank
(b) Mn(II)-PAR complex versus blank

3.4.2.2 Manifold and Procedure

The FIA manifold for the determination of Co(II) using PAR is shown in Figure 3.42. The UVIS-200 detector (LINEAR INSTRUMENTS) was used as spectrophotometer. A flow-through cell was adapted from the original HPLC style by increasing inner diameter in order to prevent the deposition of air bubble and to serve more sensitivity.

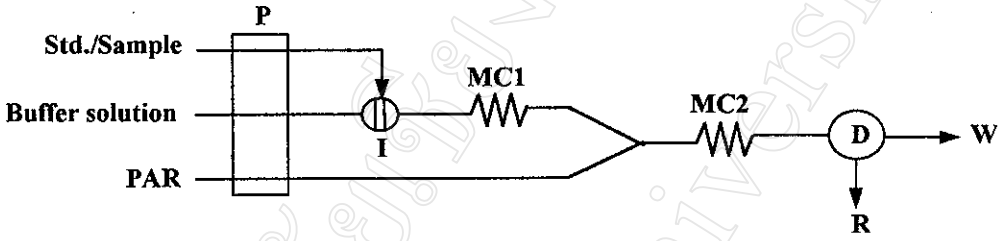

Figure 3.42 FIA manifold for the determination of Co(II) using PAR
P=peristaltic pump; I=injection valve; MC=mixing coils;
D = UVIS-200 detector; R = chart recorder; W = waste

A standard or sample is injected via a sample loop into a carrier stream of citrate buffer solution (pH 6.0). This stream passes through a mixing coil (MC1) before merging with the reagent stream of PAR. After passing through a second mixing coil (MC2), the coloured complex is then carried into a spectrophotometric flow cell, where the absorbance is continuously measured at 520 nm.

3.4.2.3 Optimization

The FIA manifold shown in Figure 3.42 was used. Preliminary conditions are shown in Table 3.54 for the optimization studied by varying one parameter while the others were kept constant.

Table 3.54 Preliminary conditions

Parameter	Condition
Buffer solution	0.060 M citrate buffer solution (pH 6.0)
PAR solution	0.0030% (w/v) PAR (in 0.060 M citrate buffer solution (pH 6.0))
Sample volume	70 µl
MC1 dimension	0.8 mm i.d. x 50 cm length
MC2 dimension	0.8 mm i.d. x 100 cm length
Flow-rate of buffer solution	1.6 ml/min
Flow-rate of PAR solution	1.6 ml/min
Analytical wavelength	475 nm
Full scale range of recorder	20 mV
Chart speed of recorder	5 mm/min

3.4.2.3.1 Mixing Coil 1 Length

The results are shown in Table 3.55 and Figure 3.43. It was found that the MC1 length was increased the peak height decreased. The irreproducible peak height was obtained when the MC1 was not used. The MC1 length of 50 cm was selected for further studies.

Table 3.55 Effect of MC1 length

Standard solution (mg Co/l)	Peak height* (mV)		
	Mixing coil 1 length (cm)		
	none	50	100
1.0	2.10	1.60	0.80
3.0	3.95	3.30	2.05
6.0	6.55	5.60	3.85
9.0	8.45	7.60	5.50
Calibration graph	y = 0.7976x + 1.4738	y = 0.7490x + 0.9673	y = 0.5878x + 0.2582
r^2	0.9931	0.9975	0.9993

*Mean of triplicate injections

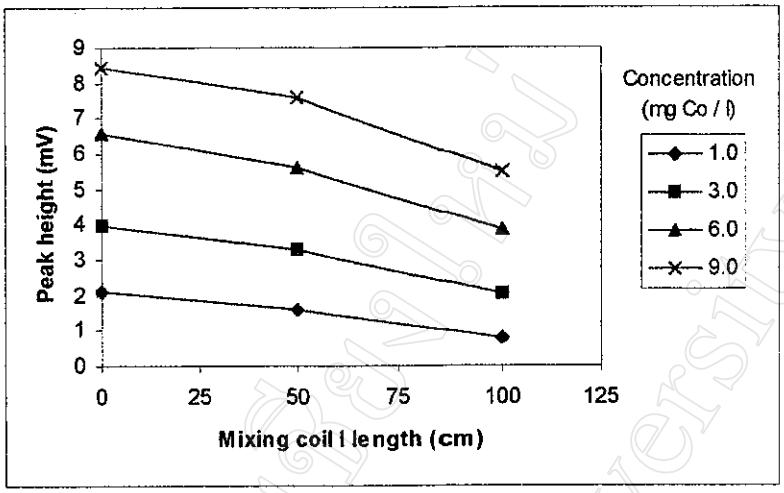

Figure 3.43 Effect of MC1 length

3.4.2.3.2 Mixing Coil 2 Length

The results are displayed in Table 3.56 and Figure 3.44. It was pointed out that the MC2 length was increased the peak height decreased. The reproducible peak height was not obtained when the MC2 length of 50 cm was used. The MC2 length of 100 cm was chosen.

Table 3.56 Effect of MC2 length

Standard solution (mg Co/l)	Peak height* (mV)		
	Mixing coil 2 length (cm)		
	50	100	150
1.0	1.95	1.60	1.15
3.0	3.60	3.30	2.50
6.0	5.70	5.60	4.60
9.0	7.60	7.60	6.50
Calibration graph	y = 0.7024x + 1.3762	y = 0.7490x + 0.9673	y = 0.6718x + 0.4966
r^2	0.9972	0.9975	0.9995

*Mean of triplicate injections

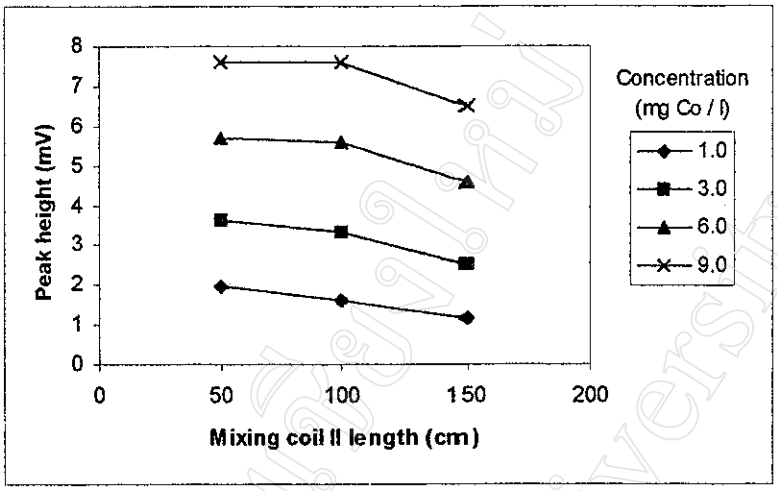

Figure 3.44 Effect of MC2 length

3.4.2.3.3 Sample Volume

The results shown in Table 3.57 and Figure 3.45 indicated that the sample volume was increased the peak height increased. The calibration graph with less r^2 value was obtained when the sample volume of 125 µl was used. The sample volume of 70 µl was selected for further studies.

Table 3.57 Effect of sample volume

Standard solution (mg Co/l)	Peak height* (mV)		
	Sample volume (µl)		
	50	70	125
1.0	1.00	1.30	2.00
3.0	2.40	3.00	4.45
6.0	4.10	5.05	7.30
9.0	5.70	6.80	9.40
Calibration graph	y = 0.5823x + 0.5340	y = 0.6827x + 0.7949	y = 0.9194x + 1.4204
r^2	0.9969	0.9941	0.9870

*Mean of triplicate injections

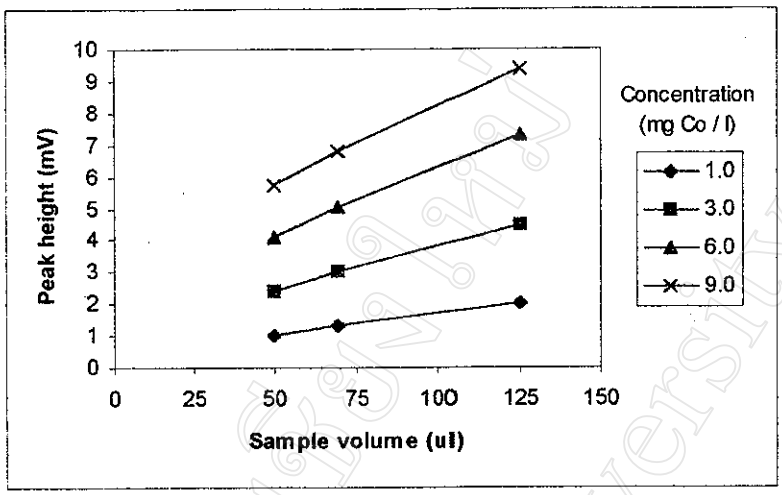

Figure 3.45 Effect of sample volume

3.4.2.3.4 Flow-rate of Buffer Solution and PAR Streams

The results are shown in Table 3.58 and Figure 3.46. It was pointed out that the rather constant peak height was obtained when the flow-rate was used in range 1.3-1.9 ml/min. The flow-rate of 1.6 ml/min was selected for both buffer solution and PAR streams.

Table 3.58 Effect of flow-rate of buffer solution and PAR streams

Flow rate (ml/min)		Peak height* (mV)				Calibration graph	r^2
Buffer solution	PAR	Standard solution (mg Co/l)					
		1.0	3.0	6.0	9.0		
1.3	1.3	1.20	3.20	5.45	7.45	y = 0.7721x + 0.6575	0.9930
1.6	1.6	1.30	3.00	5.05	6.80	y = 0.6827x + 0.7949	0.9941
1.9	1.9	1.15	2.85	4.75	6.60	y = 0.6718x + 0.6466	0.9953

*Mean of triplicate injections

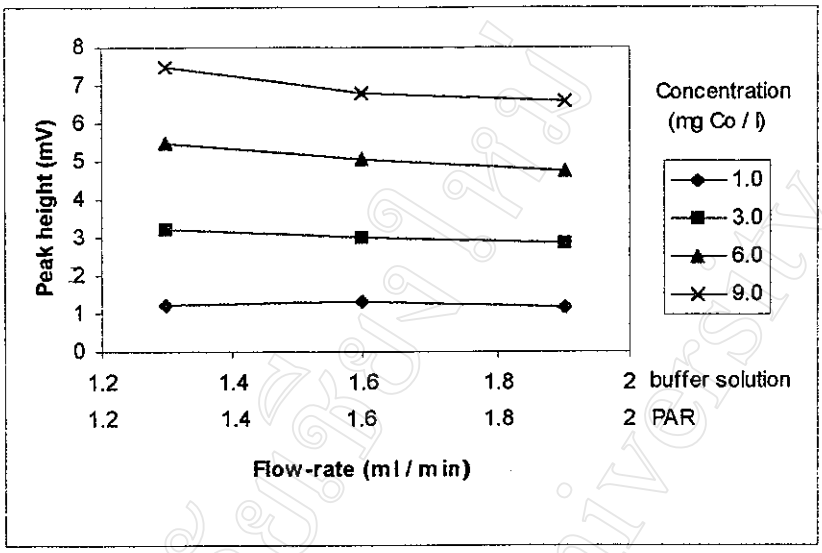

Figure 3.46 Effect of flow-rate of buffer solution and PAR streams

3.4.2.3.5 Analytical Wavelength

The results are shown in Table 3.59 and Figure 3.47. It was indicated that higher signal was obtained when the analytical wavelength of 520 nm was used instead of 475 nm. The analytical wavelength of 520 nm was chosen for further studies.

Table 3.59 Effect of analytical wavelength

Standard solution (mg Co/l)	**Peak height* (mV)**	
	Analytical wavelength (nm)	
	475	**520**
1.0	1.53	1.95
3.0	3.15	4.95
6.0	5.31	8.68
9.0	7.02	11.75
Calibration graph	y = 0.6863x + 0.9924	y = 1.2194x + 1.0404
r^2	0.9946	0.9939

*Mean of triplicate injections

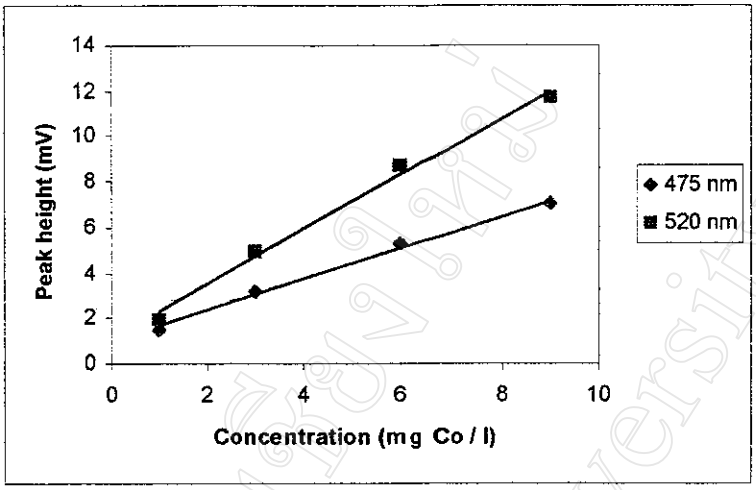

Figure 3.47 Effect of analytical wavelength

3.4.2.3.6 Concentration of PAR Solution

The results are displayed in Table 3.60 and Figure 3.48. It was indicated that the concentration of PAR solution was increased the peak height increased. The red colour of PAR solution was attached on tubing and flow-through cell when the concentration of PAR solution was used higher than 0.0030% (w/v). Baseline was risen gradually. The PAR solution concentration of 0.0030% (w/v) was chosen.

Table 3.60 Effect of concentration of PAR solution

Concentration of PAR solution (% (w/v))	Peak height* (mV) Standard solution (mg Co/l)				Calibration graph	r^2
	1.0	3.0	6.0	9.0		
0.0003	0.40	0.55	0.70	0.85	y = 0.0551x + 0.3633	0.9918
0.0007	0.55	1.05	1.65	2.00	y = 0.1813x + 0.4514	0.9765
0.0015	1.35	3.07	4.93	6.33	y = 0.6158x + 0.9950	0.9844
0.0030	1.95	4.95	8.68	11.75	y = 1.2194x + 1.0404	0.9939

*Mean of triplicate injections

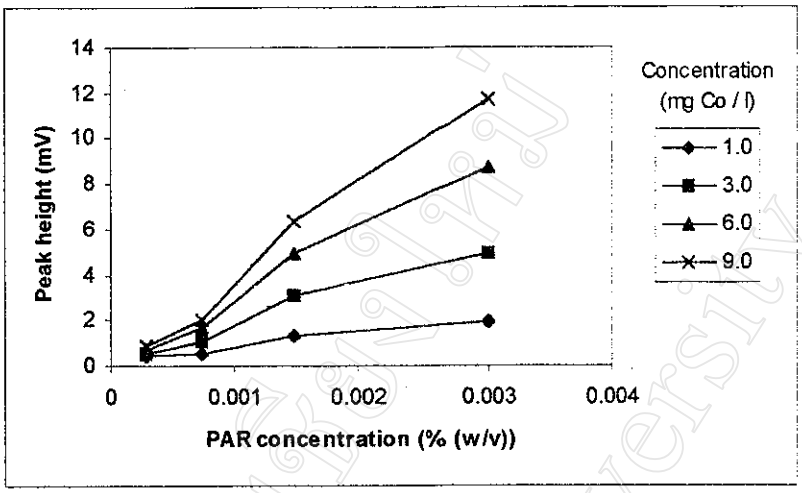

Figure 3.48 Effect of concentration of PAR solution

3.4.2.3.7 Concentration of Citrate Buffer Solution

The results are shown in Table 3.61 and Figure 3.49. It was pointed out that the concentration of citrate buffer solution was increased the peak height decreased. The splited peak was obtained when the concentration of citrate buffer solution was increased. The citrate buffer solution concentration of 0.060 M was selected.

Table 3.61 Effect of concentration of citrate buffer solution

Concentration of citrate buffer solution (M)	Peak height* (mV) Standard solution (mg Co/l)				Calibration graph	r^2
	1.0	3.0	6.0	9.0		
0.060	2.00	5.15	9.35	12.78	y = 1.3467x + 0.9233	0.9956
0.120	1.55	3.95	7.35	10.08	y = 1.0695x + 0.6526	0.9963
0.180	1.30	3.30	6.05	8.55	y = 0.9048x + 0.5024	0.9986
0.240	1.60	3.50	5.80	7.70	y = 0.7578x + 1.0503	0.9932
0.300	1.25	3.00	5.10	6.60	y = 0.6663x + 0.8224	0.9870

*Mean of triplicate injections

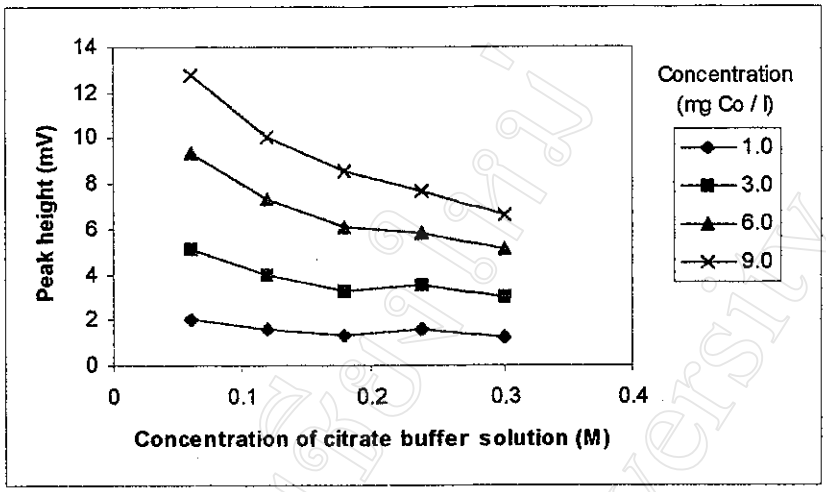

Figure 3.49 Effect of concentration of citrate buffer solution

3.4.2.4 Summary of the Optimum Conditions

The recommended FIA manifold shown in Figure 3.42 for the determination of Co(II) using PAR was optimized. The optimum conditions are summarized in Table 3.62.

Table 3.62 Optimum conditions

Parameter	Condition
Buffer solution	0.060 M citrate buffer solution (pH 6.0)
PAR solution	0.0030% (w/v) PAR (in 0.060 M citrate buffer solution (pH 6.0))
Sample volume	70 µl
MC1 dimension	0.8 mm i.d. x 50 cm length
MC2 dimension	0.8 mm i.d. x 100 cm length
Flow-rate of buffer solution	1.6 ml/min
Flow-rate of PAR solution	1.6 ml/min
Analytical wavelength	520 nm
Full scale range of recorder	20 mV
Chart speed of recorder	5 mm/min

3.4.2.5 Calibration Graph and Detection Limit

The calibration graph was accomplished by using the optimum conditions concluded in section 3.4.2.4. The detection limit ($3S_B$) was also estimated from the calibration graph [232]. The results are shown in Table 3.63 and Figures 3.50 and 3.51. The detection limit was calculated as 0.8 mg Co/l.

Table 3.63 Peak height of Co(II) standard solutions

Standard solution (mg Co/l)	Peak height* (mV)	Calibration graph
1.0	2.19	$y = 1.3458x + 1.1350$ $r^2 = 0.9963$
3.0	5.46	
6.0	9.41	
9.0	13.05	

*Mean of quadruplicate injections

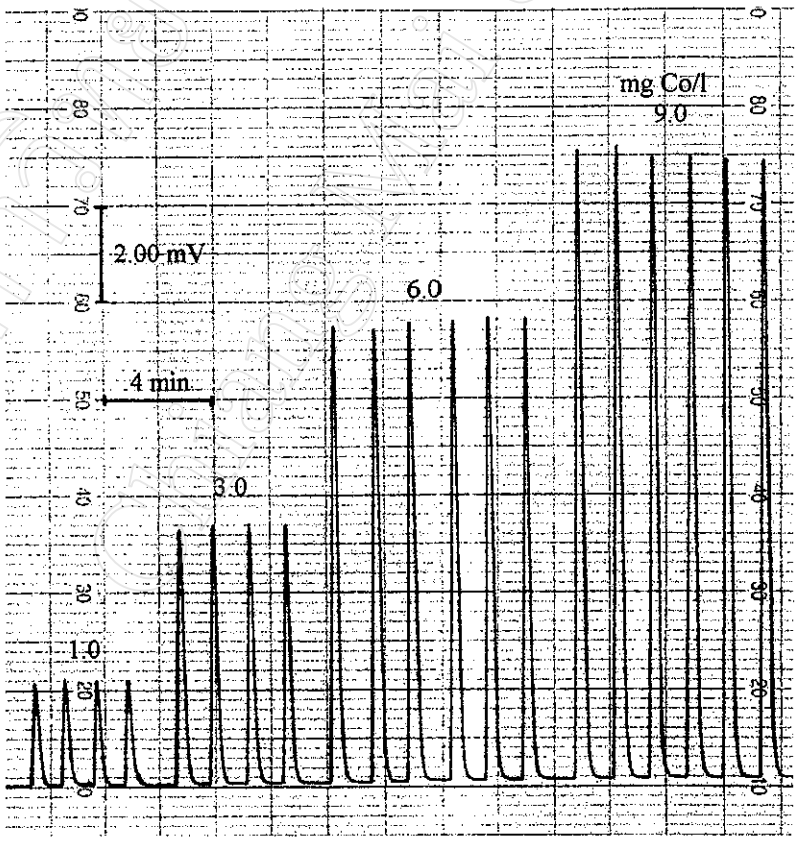

Figure 3.50 FIA-gram of Co(II) standard solution

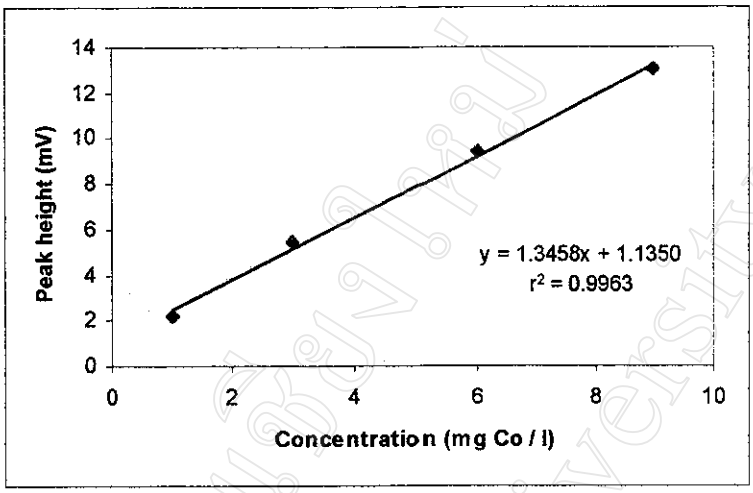

Figure 3.51 Calibration graph

3.4.2.6 Precision

The precision was determined by using the optimum conditions concluded in section 3.4.2.4. The standard solution (6.0 mg Co/l) was repeatedly injected for 11 replicates. The results are shown in Table 3.64. The relative standard deviation of 0.3% was obtained.

Table 3.64 Precision study

Standard Solution (mg Co/l)	Peak height (mV)	$\bar{x}$ (mV)	SD	%RSD
6.0	8.75, 8.75, 8.75, 8.75, 8.80, 8.70, 8.75, 8.75, 8.70, 8.80, 8.75	8.75	0.03	0.3

3.4.2.7 Ratio of Glacial Acetic Acid: Xylene: Deionized Water in Mixed Solvent

This was studied by varying the ratio of xylene and deionized water, while glacial acetic acid was kept constant, in mixed solvent for preparing of the stock standard Co(II). The stock standard 2500 mg Co/l was diluted to 600 mg Co/l with different ratios of xylene and deionized water. The little separation of xylene into upper layer occurred when the stock standard 600 mg Co/l was prepared by using mixed solvent in the

ratio of 70: 15: 15 and 70: 10: 20. The separation was not appeared when mixed solvent was used in the common ratio of 70: 22: 8. The working standard 6.0 mg Co/l was prepared by sampling the bottom layer of stock standard 600 mg Co/l and appropriate diluting with 50% (v/v) isopropanol solution. The results are displayed in Table 3.65. It was indicated that the determination of Co(II) was not effected by increasing the ratio of deionized water up to 20% by volume.

Table 3.65 Effect of the ratio of glacial acetic acid: xylene: deionized water in mixed solvent

Ratio of glacial acetic acid: xylene: deionized water (by volume) in mixed solvent	**No. (preparation of stock standard 600 mg Co/l)**	**Peak height (mV) of standard solution 6.0 mg Co/l**	**$\bar{x}$ (mV)**
70: 22: 8 (common ratio)	-	8.90, 8.90, 8.90, 9.00, 9.00, 9.00, 9.00	$\bar{x} \pm 3(SD)$ $= 8.96 \pm 3(0.05)$ $= 8.81 - 9.11$
70: 15: 15	1	9.00, 9.00, 9.00	9.00
	2	9.00, 9.00, 9.00	9.00
70: 10: 20	1	9.00, 9.00, 9.00	9.00
	2	8.95, 8.95, 8.95	8.95

3.4.2.8 Interference Study

The effect of interfering ions was studied by adding interfering ions into standard solution (6.0 mg Co/l). The concentration at which an ion would interfere is determined when a relative error of 10% of the peak height of the original solution of 6.0 mg Co/l is obtained. The results are displayed in Table 3.66. It was pointed out that concentration of Mn(II) up to 12.5 mg/l and Br^- up to 20.0 mg/l did not interfere the determination of Co(II) (6.0 mg/l).

Table 3.66 Interference study

Ion added	Added chemical form	Concentration added (mg/l)	Peak height* (mV)	% Relative error
Mn^{2+}	$Mn(OAc)_2.4H_2O$	-	8.70	-
		3.0	8.80	+ 1.1
		6.0	8.80	+ 1.1
		9.0	8.95	+ 2.9
		12.5	8.82	+ 1.4
Br^-	NH_4Br	-	8.81	-
		5.0	8.66	- 1.7
		10.0	8.79	- 0.2
		15.0	8.79	- 0.2
		20.0	8.84	+ 0.3

*Mean of triplicate injections

3.4.3 Flow-Injection Spectrophotometric Determination of Manganese(II) with Formaldoxime

The formaldoxime method has been applied extensively to the spectrophotometric determination of manganese, because of its high sensitivity and the rapid formation of a stable coloured complex. The chemical structure of formaldoxime is shown in Figure 3.52.

$$H_2C = N - OH$$

Figure 3.52 Chemical structure of formaldoxime [225]

Formaldoxime can be obtained by reaction of hydroxylammonium chloride with formaldehyde. Formaldoxime is dissociated in an alkaline medium, producing anions ($H_2C=NO^-$) that form coloured complex with multivalent metals (manganese, copper, nikel, cerium and vanadium) [225]. The pink colour produced of Mn-formaldoxime complex has a constant intensity over the pH range 9.0 to 10.5, and the absorbance is measured at 480 nm. The molar absorptivity is $1.1x10^4$ l/mol.cm [216].

3.4.3.1 Preliminary Studies: Spectral Characteristics of the Mn(II)-Formaldoxime Complex

The absorption spectra of Mn(II)-formaldoxime complex were studied. The solution containing 5.00 ml of standard solution (6.0 mg Mn/l), 5.00 ml of 9.7 M NH_4Cl/NH_4OH buffer solution (pH 10.0) and 3.00 ml of 2.0 M formaldoxime solution was prepared and diluted to 50.0 ml with water. The solution containing Co(II) standard solution instead of Mn(II) and a blank solution were also prepared. All electronic absorption spectra were recorded using a HITACHI U-200 Spectrophotometer (Japan). The recorded absorption spectra are displayed in Figure 3.53. The maximum absorption of Mn(II)-formaldoxime complex was observed at 450 nm.

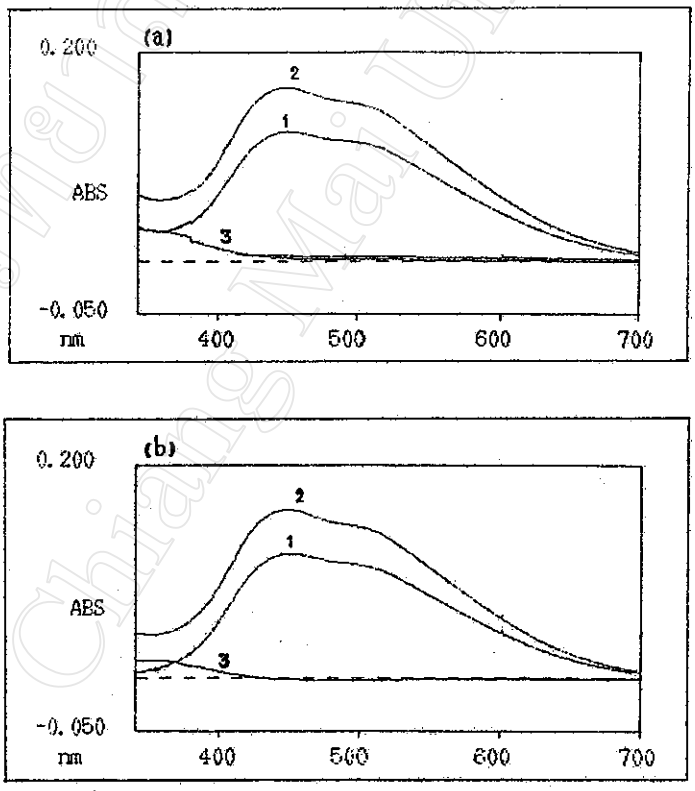

Figure 3.53 Absorption spectra versus water (a) and versus blank (b)
1 = Mn(II)-formaldoxime complex
2 = Sample in formaldoxime solution
3 = Co(II) in formaldoxime solution

3.4.3.2 Manifold and Procedure

The FIA manifold for the determination of Mn(II) using formaldoxime is shown in Figure 3.54. The same instruments used for the determination of Co(II) using PAR were also used.

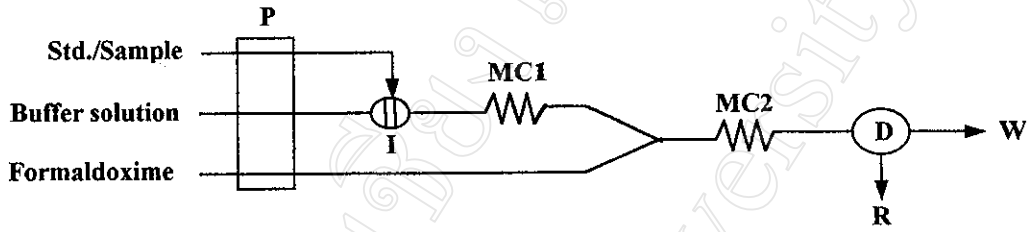

Figure 3.54 FIA manifold for the determination of Mn(II) using formaldoxime; P = peristaltic pump; I = injection valve; MC = mixing coils; D = UVIS-200 detector; R = chart recorder; W = waste

A standard or sample is injected via a sample loop into a stream of NH_4Cl/NH_4OH buffer solution (pH 10.0). This stream passes through a mixing coil (MC1) before merging with the reagent stream of formaldoxime. After passing through a second mixing coil (MC2), the coloured complex is then carried into a spectrophotometric flow cell, where the absorbance is continuously measured at 475 nm.

3.4.3.3 Optimization

The FIA manifold shown in Figure 3.54 was used. Preliminary conditions are shown in Table 3.67 for the optimization studied by varying one parameter while the others were kept constant. Attempts have been made to analyze Co(II) and Mn(II) by using the same manifold in order to obtain a rapid, simple and economic method.

Table 3.67 Preliminary conditions

Parameter	Condition
Buffer solution	9.70 M NH_4Cl/NH_4OH buffer solution (pH 10.0)
Formaldoxime	2.05 M formaldoxime solution
Sample volume	70 µl
MC1 dimension	0.8 mm i.d. x 50 cm length
MC2 dimension	0.8 mm i.d. x 150 cm length
Flow-rate of buffer solution	1.6 ml/min
Flow-rate of formaldoxime	1.6 ml/min
Analytical wavelength	475 nm
Full scale range of recorder	20 mV
Chart speed of recorder	5 mm/min

3.4.3.3.1 Mixing Coil 1 Length

The results are displayed in Table 3.68 and Figure 3.55. It was found that the MC1 length was increased the peak height decreased. The irreproducible peak height was obtained when the MC1 was not used. The MC1 length of 50 cm was chosen for further studies.

Table 3.68 Effect of MC1 length

Standard solution (mg Mn/l)	Peak height* (mV)		
	Mixing coil 1 length (cm)		
	none	50	100
1.0	0.50	0.40	0.30
3.0	1.40	1.05	0.65
6.0	2.75	2.05	1.20
9.0	3.80	2.90	1.90
Calibration graph	$y = 0.4153x + 0.1398$	$y = 0.3143x + 0.1071$	$y = 0.1990x + 0.0673$
r^2	0.9963	0.9986	0.9953

*Mean of triplicate injections

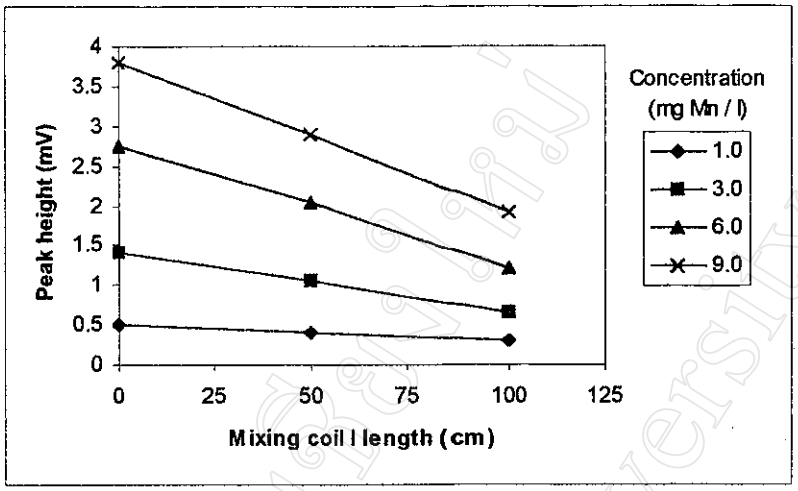

Figure 3.55 Effect of MC1 length

3.4.3.3.2 Mixing Coil 2 Length

The results shown in Table 3.69 and Figure 3.56 pointed out that the MC2 length was increased the peak height decreased. The reproducible peak height was not obtained when the MC2 length of 50 cm was used. The MC2 length of 100 cm was selected.

Table 3.69 Effect of MC2 length

Standard solution (mg Mn/l)	Peak height* (mV)		
	Mixing coil 2 length (cm)		
	50	100	150
1.0	0.40	0.40	0.25
3.0	1.10	1.05	0.70
6.0	2.15	2.05	1.60
9.0	3.20	2.90	2.50
Calibration graph	y = 0.3500x + 0.0500	y = 0.3143x + 0.1071	y = 0.2847x - 0.0898
r^2	1.0000	0.9986	0.9972

*Mean of triplicate injections

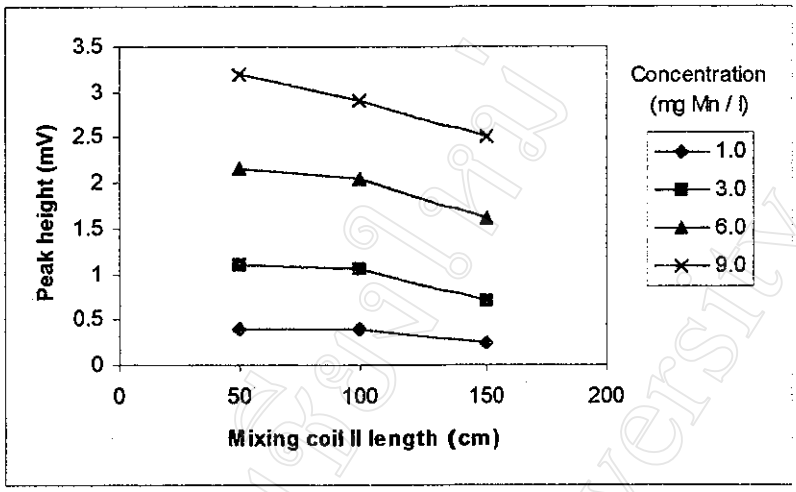

Figure 3.56 Effect of MC2 length

3.4.3.3.3 Sample Volume

The results are shown in Table 3.70 and Figure 3.57. It was indicated that the sample volume was increased the peak height increased. The splited peak was obtained when the sample volume of 125 µl was used. The sample volume of 70 µl was selected for further studies.

Table 3.70 Effect of sample volume

Standard solution (mg Mn/l)	**Peak height* (mV)**		
	Sample volume (µl)		
	50	**70**	**125**
1.0	0.20	0.40	0.50
3.0	0.60	1.05	1.60
6.0	1.20	2.05	3.00
9.0	1.80	2.90	4.20
Calibration graph	y = 0.2000x – 0.0000	y = 0.3143x + 0.1071	y = 0.4605x + 0.1374
r^2	1.0000	0.9986	0.9958

*Mean of triplicate injections

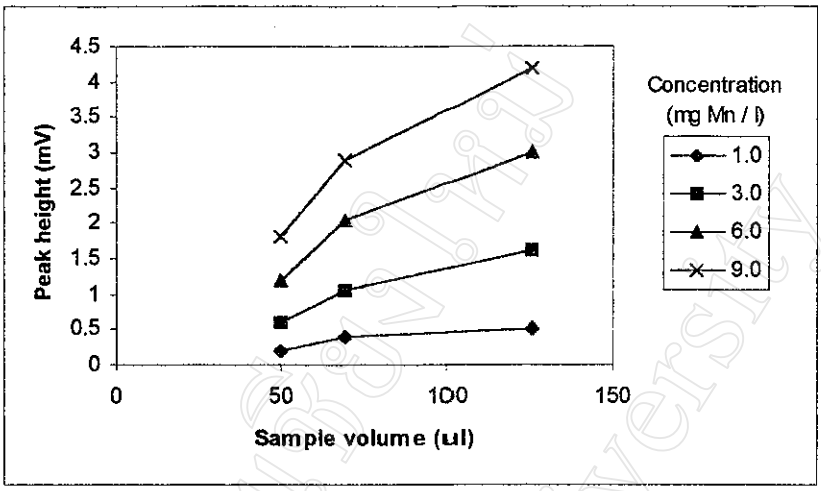

Figure 3.57 Effect of sample volume

3.4.3.3.4 Flow-rate of Buffer Solution and Formaldoxime Streams

The results are displayed in Table 3.71 and Figure 3.58. It was pointed out that the flow-rate was increased the peak height decreased. The broad peak was obtained when the flow-rate of 0.8 ml/min was used. The flow-rate of 1.6 ml/min was selected for both buffer solution and formaldoxime streams.

Table 3.71 Effect of flow-rate of buffer solution and formaldoxime streams

Flow rate (ml/min)		Peak height* (mV)				Calibration graph	r^2
Buffer solution	Formaldoxime	Standard solution (mg Mn/l)					
		1.0	3.0	6.0	9.0		
0.8	0.8	0.55	1.10	2.30	3.40	y = 0.3629x + 0.1136	0.9966
1.6	1.6	0.40	1.05	2.05	2.90	y = 0.3143x + 0.1071	0.9986
2.2	2.2	0.30	0.80	1.75	2.60	y = 0.2915x - 0.0221	0.9987

*Mean of triplicate injections

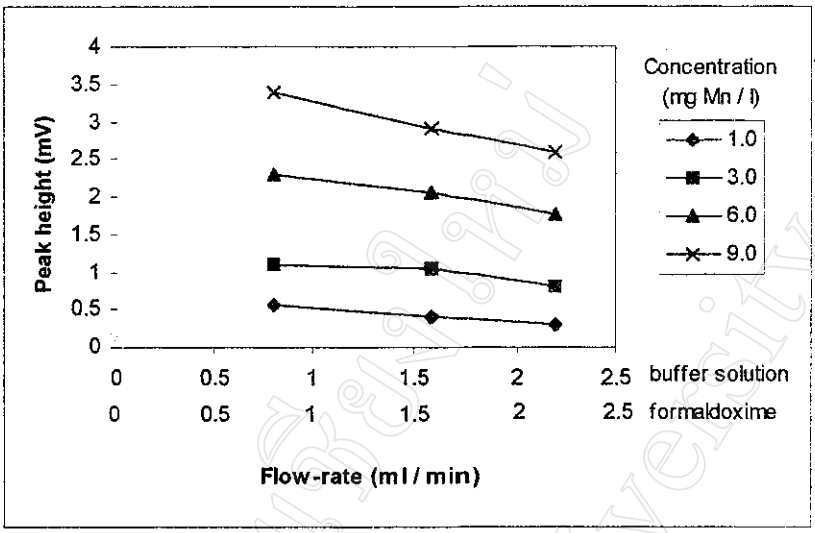

Figure 3.58 Effect of flow-rate of buffer solution and formaldoxime streams

3.4.3.3.5 Concentration of NH_4Cl/NH_4OH Buffer and Formaldoxime Solutions

This was studied by diluting the NH_4Cl/NH_4OH buffer and formaldoxime solutions with water. The results are shown in Table 3.72 and Figure 3.59. It was found that the rather constant peak height was obtained when the concentration of NH_4Cl/NH_4OH buffer (pH 10.0) and formaldoxime solutions were used higher than 1.45 M and 0.31 M respectively. The peak height was decreased when the concentration of NH_4Cl/NH_4OH buffer and formaldoxime solutions were used at 0.97 M and 0.20 M respectively. The concentration of 1.94 M was chosen for NH_4Cl/NH_4OH buffer solution (pH 10.0).

Table 3.72 Effect of concentration of NH_4Cl/NH_4OH buffer and formaldoxime solutions

Concentration (M) of		Peak height* (mV)				Calibration graph	r^2
NH_4Cl/NH_4OH buffer solution	Formaldoxime solution	Standard solution (mg Mn/l)					
		1.0	3.0	6.0	9.0		
9.70	2.05	0.30	0.85	1.90	2.85	$y = 0.3231x - 0.0599$	0.9986
4.85	1.02	0.30	0.80	1.77	2.65	$y = 0.2980x - 0.0353$	0.9984
2.42	0.51	0.20	0.78	1.73	2.60	$y = 0.3020x - 0.1069$	0.9997
1.94	0.41	0.30	0.83	1.77	2.57	$y = 0.2873x + 0.0029$	0.9988
1.45	0.31	0.30	0.80	1.70	2.47	$y = 0.2748x + 0.0124$	0.9988
0.97	0.20	0.25	0.60	1.38	2.00	$y = 0.2241x - 0.0072$	0.9961

*Mean of triplicate injections

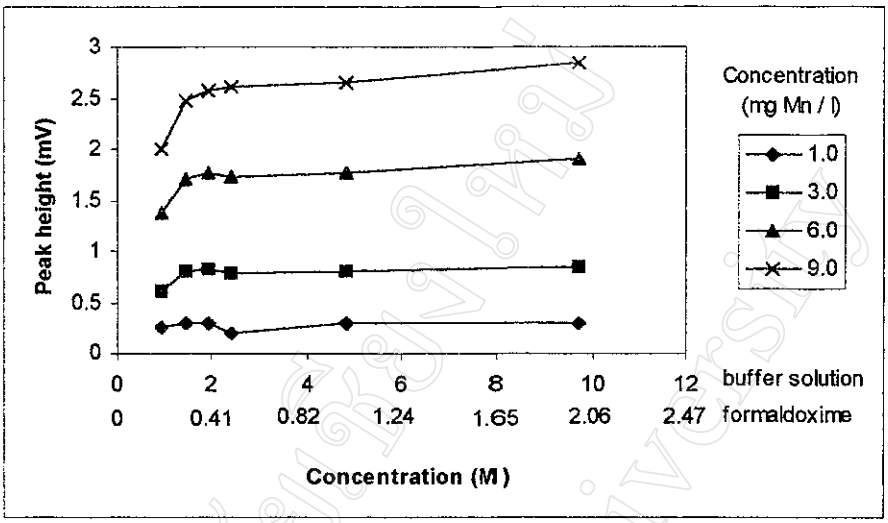

Figure 3.59 Effect of concentration of NH_4Cl/NH_4OH buffer and formaldoxime solutions

The effect of concentration of formaldoxime solution was further studied. The results are displayed in Table 3.73 and Figure 3.60. It was found that the rather constant peak height was obtained when the concentration of formaldoxime solution was used higher than 0.10 M. The peak height was decreased when the concentration of 0.05 M was used. The concentration of 0.20 M was selected for formaldoxime solution.

Table 3.73 Effect of concentration of formaldoxime solution

Concentration of formaldoxime solution (M)	Peak height* (mV) Standard solution (mg Mn/l)				Calibration graph	r^2
	1.0	3.0	6.0	9.0		
0.31	0.30	0.80	1.70	2.47	y = 0.2748x + 0.0124	0.9988
0.20	0.25	0.80	1.68	2.58	y = 0.2919x - 0.0590	0.9997
0.10	0.25	0.75	1.57	2.37	y = 0.2663x - 0.0297	0.9998
0.05	0.20	0.40	0.75	1.10	y = 0.1133x + 0.0745	0.9991

*Mean of triplicate injections

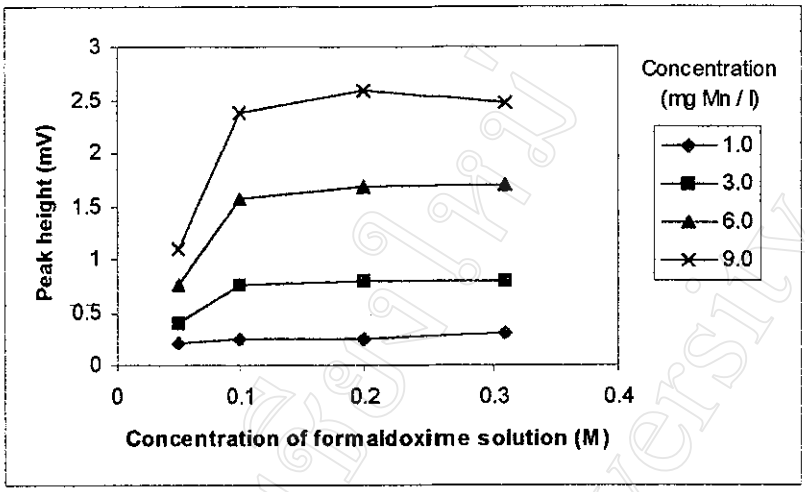

Figure 3.60 Effect of concentration of formaldoxime solution

3.4.3.4 Summary of the Optimum Conditions

The proposed FIA manifold shown in Figure 3.54 for the determination of Mn(II) using formaldoxime was optimized. The optimum conditions are concluded in Table 3.74.

Table 3.74 Optimum conditions

Parameter	Condition
Buffer solution	1.94 M NH_4Cl/NH_4OH buffer solution (pH 10.0)
Formaldoxime	0.20 M formaldoxime solution
Sample volume	70 µl
MC1 dimension	0.8 mm i.d. x 50 cm length
MC2 dimension	0.8 mm i.d. x 100 cm length
Flow-rate of buffer solution	1.6 ml/min
Flow-rate of formaldoxime	1.6 ml/min
Analytical wavelength	475 nm
Full scale range of recorder	20 mV
Chart speed of recorder	5 mm/min

3.4.3.5 Calibration Graph and Detection Limit

The calibration graph was executed by using the optimum conditions concluded in section 3.4.3.4. The detection limit was also estimated from the calibration graph. The results are shown in Table 3.75 and Figures 3.61 and 3.62. The detection limit ($3S_B$) [232] was calculated as 0.2 mg Mn/l.

Table 3.75 Peak height of Mn(II) standard solutions

Standard solution (mg Mn/l)	Peak height* (mV)	Calibration graph
1.0	0.35	$y = 0.3174x + 0.0473$ $r^2 = 0.9998$
3.0	1.02	
6.0	1.95	
9.0	2.90	

*Mean of triplicate injections

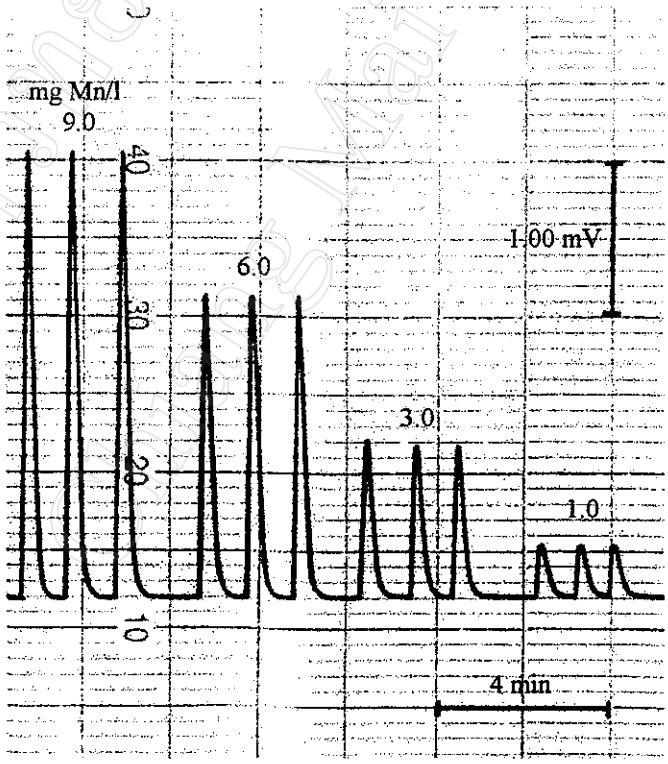

Figure 3.61 FIA-gram of Mn(II) standard solutions

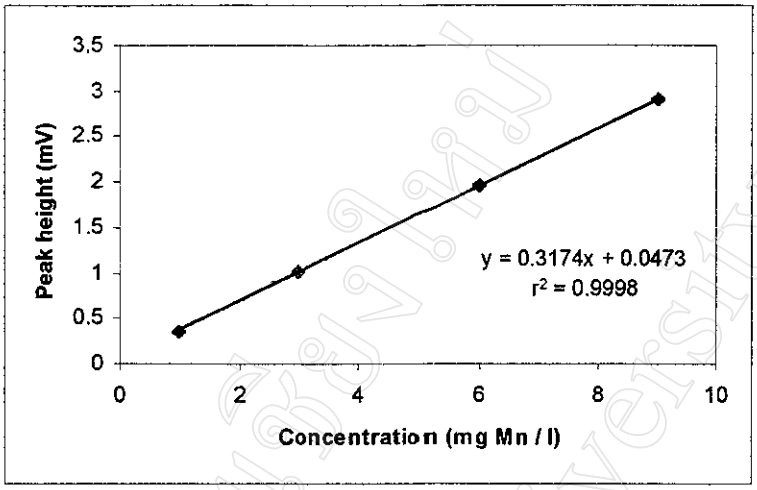

Figure 3.62 Calibration graph

3.4.3.6 Precision

The precision was determined by using the optimum conditions summarized in section 3.4.3.4. The standard solution (6.0 mg Mn/l) was repeatedly injected for 11 replicates. The results are displayed in Table 3.76. The relative standard deviation of 2.3% was obtained.

Table 3.76 Precision study

Standard Solution (mg Mn/l)	Peak height (mV)	$\bar{x}$ (mV)	SD	%RSD
6.0	1.70, 1.78, 1.78, 1.78, 1.78, 1.78, 1.70, 1.70, 1.70, 1.70, 1.70	1.74	0.04	2.3

3.4.3.7 Ratio of Glacial Acetic Acid: Xylene: Deionized Water in Mixed Solvent

This was studied by varying the ratio of xylene and deionized water, while glacial acetic acid was kept constant, in mixed solvent for preparing of the stock standard Mn(II). The stock standard 2500 mg Mn/l was diluted to 600 mg Mn/l with different ratios of xylene and deionized water. The little separation of xylene into upper layer occurred when the stock standard 600 mg Mn/l was prepared by using mixed solvent in the ratio of 70: 15:15 and 70: 10: 20. The separation was not appeared when

mixed solvent was used in the common ratio of 70: 22:8. The working standard 6.0 mg Mn/l was prepared by sampling the bottom layer of stock standard 600 mg Mn/l and appropriate diluting with 50% (v/v) isopropanol solution. The results shown in Table 3.77 indicated that the determination of Mn(II) was not effected by increasing the ratio of deionized water up to 20% by volume.

Table 3.77 Effect of the ratio of glacial acetic acid: xylene: deionized water in mixed solvent

Ratio of glacial acetic acid: xylene: deionized water (by volume) in mixed solvent	**Peak height (mV) of standard solution 6.0 mg Mn/l**	$\bar{x}$ **(mV)**
70: 22: 8 (common ratio)	1.70, 1.78, 1.78, 1.78, 1.78, 1.78 1.70, 1.70, 1.70, 1.70, 1.70	$\bar{x} \pm 3(SD)$ $= 1.74 \pm 3(0.04)$ $= 1.62 - 1.86$
70: 15: 15	1.88, 1.85, 1.85, 1.85, 1.85, 1.78 1.80, 1.80, 1.80	1.83
70: 10: 20	1.78, 1.78, 1.78, 1.78, 1.78, 1.75 1.75, 1.75, 1.75	1.77

3.4.3.8 Interference Study

The effect of interfering ions was studied by adding interfering ions into standard solution (6.0 mg Mn/l). The concentration at which an ion would interfere is determined when a relative error of 10% of the peak height of the original solution of 6.0 mg Mn/l is obtained. The results are listed in Table 3.78. It was indicated that concentration of Co(II) up to 12.5 mg/l and Br^- up to 20.0 mg/l did not interfere the determination of Mn(II) (6.0 mg/l).

Table 3.78 Interference study

Ion added	Added chemical form	Concentration added (mg/l)	Peak height* (mV)	% Relative error
Co^{2+}	$Co(OAc)_2.4H_2O$	-	1.75	-
		3.0	1.73	- 1.1
		6.0	1.70	- 2.8
		9.0	1.69	- 3.4
		12.5	1.75	0
Br^-	NH_4Br	-	1.50	-
		5.0	1.50	0
		10.0	1.50	0
		15.0	1.48	- 1.3
		20.0	1.46	- 2.7

*Mean of triplicate injections

3.4.4 Determination of Co(II) and Mn(II) in Reused Catalyst Sample

The FIA procedure with the optimum conditions summarized in section 3.4.2.4 and 3.4.3.4 were applied to determine contents of Co(II) and Mn(II) respectively in reused catalyst samples. Appropriated dilutions with 50% (v/v) isopropanol solution were made before injection into the FIA system. Co(II) and Mn(II) contents were obtained via its calibration graph.

The results are shown in Table 3.79. The ICP-AES was also used to determine Co(II) and Mn(II) contents in these samples. The differences between the means obtained from the recommended FIA method and the reference method were evaluated by t-test. The calculated t-test values of the recommended FIA and ICP-AES methods were 0.439 and 1.463 for the determination of Co(II) and Mn(II) respectively. The critical value of t-test is 1.734 (18 degrees of freedom) at the confidence interval of 90% [232]. It was indicated that the results obtained by the recommended methods were not significantly different from those obtained by the ICP-AES method with confidence interval of 90%.

Table 3.79 Determination of Co(II) and Mn(II) in reused catalyst samples

Sample	No. (Analysis)	Co(II) content (mg Co/l)		Mn(II) content (mg Mn/l)	
		FIA	ICP-AES	FIA	ICP-AES
A	1	534	569	573	561
	2	542		569	
	3	534		530	
B	1	529	582	542	581
	2	542		526	
C	1	530	571	566	575
	2	526		553	
	3	530		518	
D	1	530	580	588	544
	2	562		576	
E	1	457	462	400	416
	2	471		411	
F	1	485	429	422	422
	2	479		426	
G	1	485	461	426	443
H	1	504	441	456	421
	2	495		418	
I	1	482	452	392	431
	2	485		407	